UNIVERSITÀ POLITECNICA DELLE MARCHE

Master Degree in Biomedical Engineering

Ectopic Focus Identification for Catheter Ablation of Atrial Fibrillation using Electoanatomical Mapping System

Tutor: Prof. Burattini Laura

Thesis of: Pallotta Luca

Co-Tutor: Dott. Sbrollini Agnese

Academic Year 2019 – 2020

ABSTRACT

Identifying the ectopic foci that activate and maintain atrial fibrillation is one of the main problems to be addressed in the treatment of the arrhythmia. It is therefore of fundamental importance to find an index that allows to precisely locate the area of interest to be treated.

The heart is a hollow muscular organ with the function of generating the force that pumps blood through blood vessels throughout the body. It can be considered as a functional syncytium, electrical and mechanical, as the heart muscle cells allow a single action potential to pass through the heart causing it to contract adequately. The contractions are triggered by signals originating from particular cells called pacemaker cells. Specifically, the action potential is initiated in the SA node, from which travels to the AV node, runs through the walls of the atria and then propagates in all the heart.

Disturbances in pulse formation, pacemaking, or conduction are heart conditions called cardiac arrhythmias. Among these is atrial fibrillation, one of the most common arrhythmias in the world characterized by a rapid and irregular heart rhythm, caused by the presence of multiple waves resulting from small chaotic re-entries, called ectopic foci, that occur in the venous structures adjacent to the atrial chambers, in particular the ostia of the pulmonary veins. The main consequence of this type of arrhythmias is that atria are unable to contract properly and the atrioventricular node is subject to multiple electrical stimuli causing an irregular transmission of impulses to the ventricles. The diagnosis of atrial fibrillation is performed through an arrhythmological examination by the analysis of ECG traces, characterized by an irregular baseline due to the small re-entry circuits. The main indicators of atrial fibrillation are the absence of P waves related to atrial depolarization, the presence of f waves between QRS complexes and irregular R-R intervals.

In recent years, catheter ablation has become the leading treatment strategy for complex arrhythmias such as atrial fibrillation. The procedure consists in introducing a small catheter or applicator into the body, aided by an image guidance system (e.g. CT, US, MRI) and once the target is located, energy is delivered to the tip of the applicator isolating and treating the tissue. It can be based on two different operating principles in relation to the type of abnormal heart rhythm to be treated: radiofrequency ablation, which uses thermal energy to create an irreversible scar; cryoablation, which uses very cold temperatures to injure myocardial tissue.

The exact location of the targets takes place via three-dimensional electroanatomical mapping systems, which allows to identify the temporal and spatial distribution of the myocardial electrical potential during a particular heart rhythm without excessive use of radiation. A mapping catheter acquires information recording the localization of the lead, of the intracavitary ECG and of other variables, in order to reconstruct in real time a 3D representation of the geometry of the cardiac chamber. A color-coded map of the activation and the voltage in different areas of the myocardium is obtained.

In order to find an alternative indicator with respect to the f wave dominant frequencies, such as the area of the spectrum, two subjects with atrial fibrillation were used. The body surface potential mapping signals and the intracardiac signals of the atria were simultaneously recorded. The electroanatomical mapping system used is the CARTO system (CARTO XP, version 7.7; Biosense-

Webster). Patients were given an adenosine bolus which blocks the atrioventricular node, allowing the easier identification of f waves dominant frequency. The dominant frequencies were obtained by calculating the maximum frequency in the band between 4-10 Hz, instead the spectral area by calculating the area of the spectrum in the same band. Having assumed the dominant frequencies as the gold standard, the activation maps were reconstructed using the respective values of the spectral areas. The results obtained appear to be consistent with the activation maps of the dominant frequencies and the literature, identifying the ectopic sites near the right atrium, with progressively decreasing activation frequencies towards the pulmonary veins.

Therefore, the spectral area of intracardiac signals could represent a new valid index for the identification of ectopic focuses that trigger atrial fibrillation, easy to calculate, less prone to disturbances and much more sensitive than the dominant frequencies.

INDEX

INTRODUCTION

Atrial fibrillation is one of the most common arrhythmias in the world that can lead to serious complications in affected individuals. It mainly affects men and whites, compared to women and blacks. The incidence is also closely linked to age, with a prevalence ranging between 0.4% and 1% in the general population and which increases exponentially. Starting from the age of 50, the prevalence of AF doubles for each subsequent decade of life: from 0.5% in the decade between 50 and 59 years, it passes to 5-7% in the decade between 70 and 79 years, to pass finally to 8-10% in the age group > 80 years.

Atrial fibrillation is a supraventricular arrhythmia characterized by a rapid and irregular heart rhythm, caused by the presence of multiple waves resulting from small chaotic re-entries that occur within the atria. The origin and maintenance of this type of disorder may be due to the activation of ectopic foci in the venous structures adjacent to the atrial chambers, in particular the ostia of the pulmonary veins.

As a main consequence of this type of arrhythmias, the atria are unable to contract properly and the atrioventricular node is subject to multiple electrical stimuli causing an irregular transmission of impulses to the ventricles. The result is therefore a reduced contractile capacity of the myocardium of the heart and a consequent difficulty in pumping blood throughout the body, an alteration of the cardiac output, possibility of thrombus formation and therefore risk of stroke.

Patients with atrial fibrillation are often asymptomatic and are diagnosed following cardiac examinations. The main symptoms of atrial fibrillation are palpitations, irregular pulse, vague chest discomfort, dizziness, fainting or symptoms of heart failure, such as weakness or shortness of breath. They can be episodic or quite frequent, especially during physical exertion, and they greatly depend on the patient's clinical condition.

The diagnosis of atrial fibrillation is performed through an arrhythmological examination by the analysis of ECG traces, characterized by an irregular baseline due to the small re-entry circuits. The main indicators of atrial fibrillation are the absence of P waves related to atrial depolarization, the presence of f waves between QRS complexes and irregular R-R intervals.

The primary treatment strategies for atrial fibrillation are ventricular frequency control, rhythm control, and catheter ablation. For some decades the latter has been very successful, being especially useful for patients in whom it is not possible to use drugs to control the rhythm or who have aggravated heart failure. Catheter ablation is a minimally invasive procedure capable of reducing the number of episodes by isolating (ablating) the abnormal electrical pathways present in cardiac tissues.

The procedure consists in introducing a small catheter or applicator into the body, aided by an image guidance system (e.g. CT, US, MRI) and once the target is located, energy is delivered to the tip of the applicator isolating and treating the tissue.

Catheter ablation can be based on two different operating principles in relation to the type of abnormal heart rhythm to be treated: radiofrequency ablation, which uses thermal energy to create an irreversible scar; cryoablation, which uses very cold temperatures to injure myocardial tissue.

The real revolution in the catheter ablation sector are the three-dimensional electroanatomical mapping systems (3D-EAM), which to date have become indispensable tools to guide the ablative therapies of arrhythmia as they are able to identify the temporal and spatial distribution of the myocardial electrical potential during a particular heart rhythm without excessive use of radiation.

A mapping catheter is used which, as it moves within the heart, acquires information about the targets needed for ablation. These systems allow the recording of the localization of the lead, of the intracavitary ECG and of other variables, in order to reconstruct in real time a 3D representation of the geometry of the cardiac chamber in question and to code with color maps the activation and the voltage in different areas of the myocardium.

From the literature it emerged that f waves dominant frequency, usually present in the frequency band between 4-10 Hz, is a valid indicator to identify the ectopic focuses of atrial fibrillation although its amplitude may vary from patient to patient. The aim of the present thesis is to find an alternative indicator with respect to frequencies, such as the area of the spectrum, that is precise and less prone to disturbances for the identification of ectopic sites that give rise to atrial fibrillation.

Furthermore, the presence of a relationship between the acquisitions of the body surface potentials, obtained by means of a normal electrocardiograph, and the acquisitions of the epicardial potentials of the heart chambers, obtained with electroanatomical mapping systems was evaluated. The search for correlation between the two potentials is also known as the inverse problem of electrocardiography, and attempts are made to calculate epicardial potentials from known body surface potentials.

1. CARDIOVASCULAR SYSTEM

1.1 CIRCULATION

The circulatory or cardiovascular system can be considered as the transport system of our body. It consists of three main components: the heart – a muscular pump; the blood vessels – a series of distributing and collecting tubes; the blood – a fluid that carries substances to and from the cells.

The circulatory system, shown in *Figure 1*, can be divided in: *pulmonary circuit*, which comprises all blood vessels within the lungs and those connecting the lungs with the heart, and *systemic circuit*, which comprises the rest of the blood vessels. The right heart supplies blood to the pulmonary circuit, whereas the left heart supplies blood to the systemic circuit.

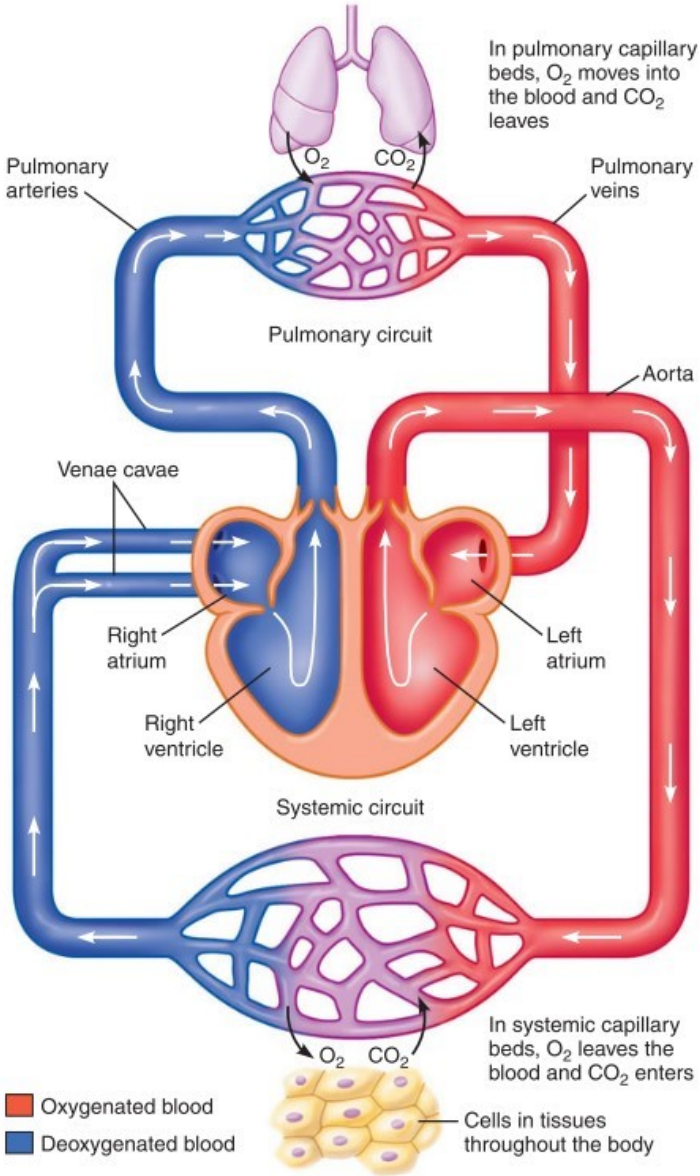

Figure 1: **The cardiovascular system.** The path of blood flow (indicated by arrows) through the pulmonary and systemic circuits is represented [1].

The dense networks of capillaries allow the exchange of nutrients and gasses (oxygen and carbon dioxide). In pulmonary capillaries, oxygen (O_2) moves into the blood from air in the lungs while carbon dioxide (CO_2) leaves the blood. The blood leaving pulmonary capillaries is rich in oxygen and

is called oxygenated blood. Systemic capillaries are found in organs and tissues that consume oxygen, which will come out of the blood, and generate carbon dioxide, which will enter it. Blood leaving the systemic capillaries is called deoxygenated blood.

As blood flows within the cardiovascular system, it travels through the pulmonary and systemic circuits in an alternating fashion, returning to the heart each time.

The left ventricle pumps oxygenated blood through the aortic valve into the aorta, carrying blood to capillary beds of all organs and tissues. Deoxygenated blood then travels back to the right atrium through the venae cavae. The superior vena cava carries blood from parts of the body above the diaphragm, whereas the inferior vena cava carries blood from parts below the diaphragm. From the right atrium blood passes to the right ventricle, which in turn pumps it into the pulmonary arteries, carrying deoxygenated blood to the lungs. The pulmonary arteries are the only arteries in the body carrying deoxygenated blood. Blood becomes oxygenated in the lungs and then travels to the left atrium in the pulmonary veins. These are the only veins in the body carrying oxygenated blood. From the left atrium, blood passes through the bicuspid valve into the left ventricle, which is where it started. The whole cycle then repeats [1].

1.2. ANATOMY OF THE HEART

The heart is asymmetrically positioned in the thoracic cavity (predominantly on the left side), as shown in *Figure 2*, between the lungs and just above the diaphragm, that separates it from the abdominal cavity. The heart has a conical shape with the apex pointing down and to the left and right ventricle more frontally positioned. Weighs approximately 300–350 g in males and 250–300 g in females. The pericardium is a thin membrane surrounding the heart and containing pericardial lubricating fluid, that prevent friction during heartbeat.

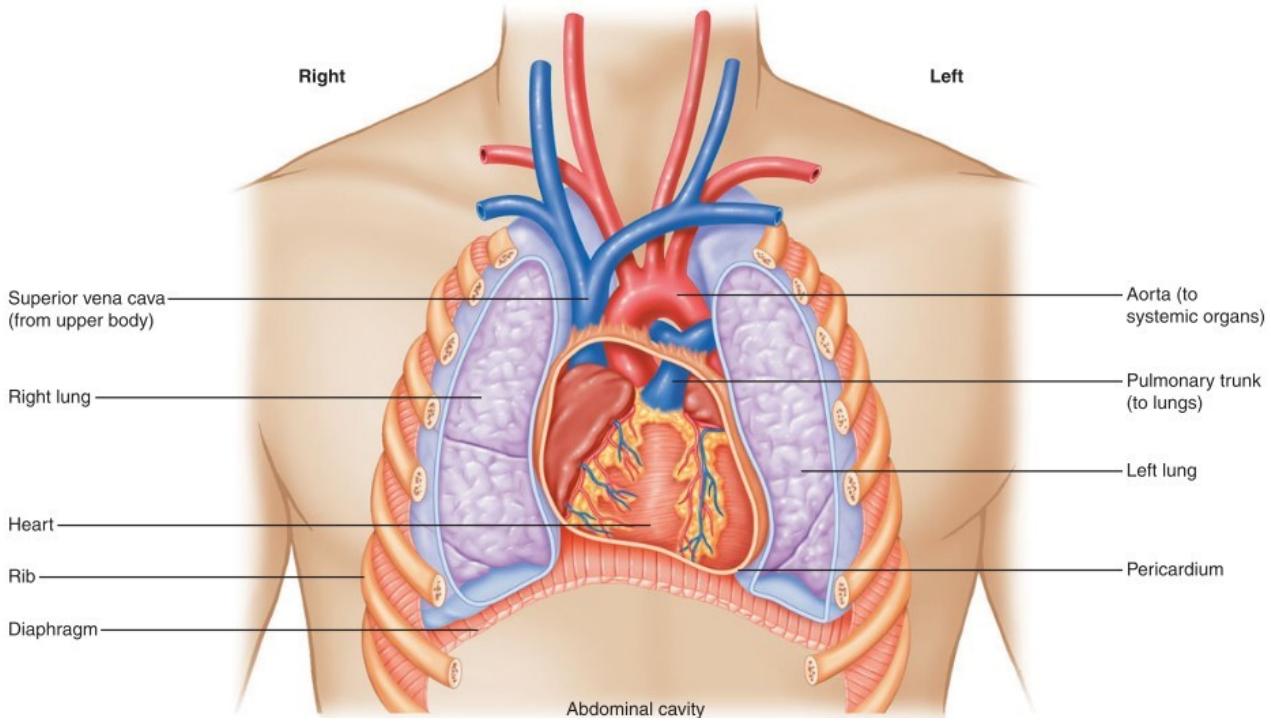

Figure 2: **Position of the heart** [1].

The heart is a hollow muscular organ with the function of generating the force that pumps blood through the blood vessels. It can be divided into two sections separated by a septum and each section includes two superimposed cavities communicating with each other. The two upper chambers, called *atria*, receive blood that comes back to the heart from the vasculature and two lower chambers, called *ventricles*, receive blood from the atria and generate the force that pushes the blood away toward blood vessels [2].

The fibrous skeleton of the heart is an internal structure made up of fibrous connective tissue that performs a dual function: it acts as the attachment site of the various muscular structures that make up the myocardium of the heart chambers, and at the same time, isolates them electrically, thus regulating the cardiac cycle according to which the atria contract first, followed by the ventricles. The fibrous skeleton also forms rings that anchor the heart valves in place.

The heart has four valves that allow blood to flow in the right direction within the heart itself and between the heart and the vessels of the body (*Figure 3*).

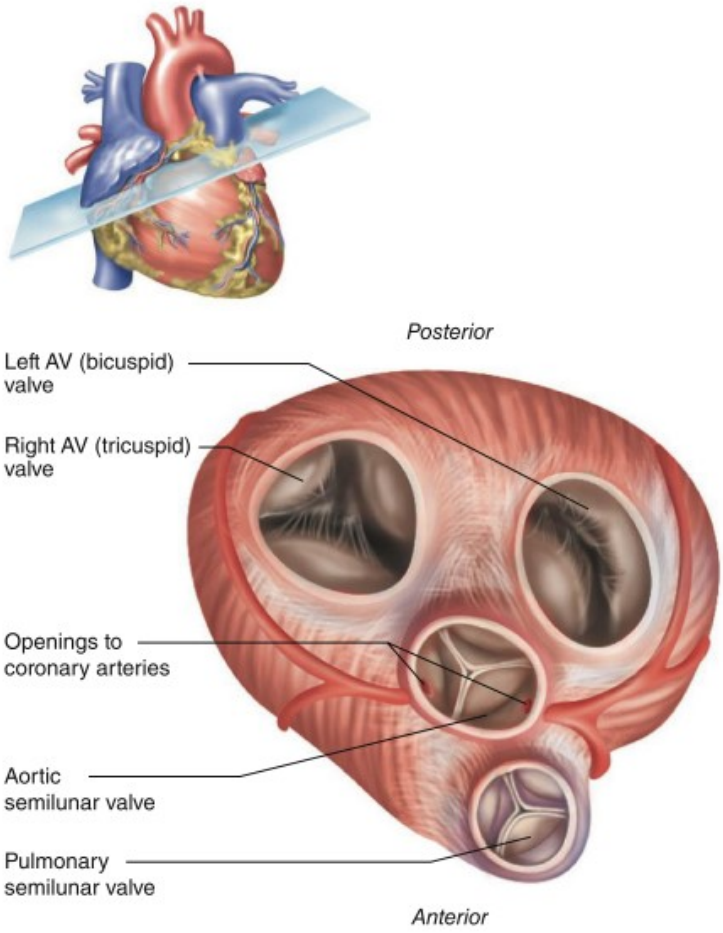

Figure 3: **Superior view of the heart with the atria removed, showing the heart valves** [3]**.**

Each atrium can communicate with the corresponding ventricle through atrioventricular (AV) valves, which allow blood to flow from the atrium to the ventricle avoiding reflux. The AV valves open and close as the pressure inside the chambers varies with each heartbeat. The left AV valve is made up of two connective tissue cusps and is therefore called the bicuspid valve or mitral valve. The right AV valve has three cusps and is called the tricuspid valve. The valve cusps are held in place by threads

of connective tissue, called tendon cords, that extend from the edges of the cusps to the papillary muscles of the ventricular wall. During the contraction, the papillary muscles also contract, exerting tension on the tendon cords and consequently allowing the AV valves to seal properly and resist the force exerted by the ventricular pressure. In addition to the AV valves, there are other valves, called semilunar valves, which are located between the ventricles and arteries. The aortic valve is located between the left ventricle and the aorta while the pulmonary valve is located between the right ventricle and the pulmonary trunk. The function of these valves is similar to that of the AV valves, namely, to prevent a change in the direction of blood flow [3].

The heart consists of three layers. The outer layer that covers the surface of the heart, is called the epicardium, and is made of connective tissue. Under the epicardium there is a thick muscular layer, the myocardium, which contracts rhythmically, allowing the function of pump. Finally, the inside of the heart is lined with a membrane called the endocardium, which covers the inner walls and heart valves and continues into inner walls of arteries and veins (endothelium).

There is a difference in the thickness of the walls of the atria and ventricles that reflects their action. Indeed, the ventricles must pump the blood over relatively longer distances through the vasculature with respect to the atria, that move blood just into the next chamber. There is also a difference in thickness between the two ventricles, as shown in *Figure 4*. In particular, the left ventricle has to pump blood to all the organs of the body except the lungs, while the right ventricle pumps blood only to the lungs, and for this it has to exert more pressure resulting in the thicker of the two [4].

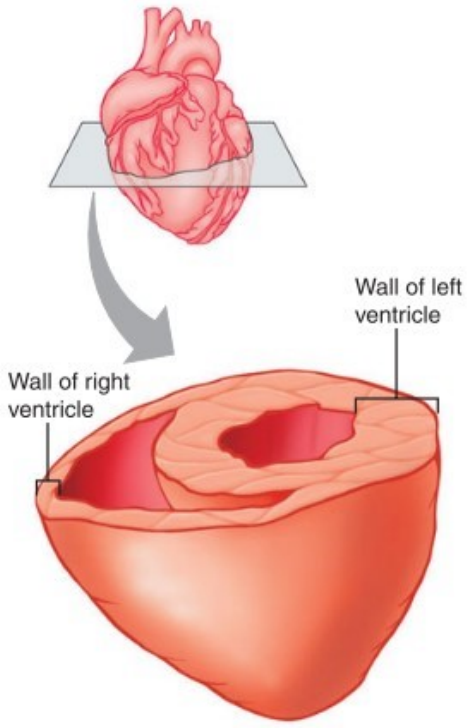

Figure 4: **Difference in thickness of the right and left ventricle** [1]**.**

1.3. ELECTRICAL ACTIVITY OF THE HEART

1.3.1. THE CONDUCTION SYSTEM

Heart walls are composed by cardiac muscle tissue, present only into the heart. All cardiac cells are connected to each other through intercalated disks, consisting of a combination of mechanical junctions and electrical connections (*Figure 5*). Desmosomes and the fascia adherents allow the mechanical connections, by keeping the cells from pulling apart when contracting. Instead, the gap junctions between the cells of the heart muscle constitute the electrical connections between the cells to allow the electrical potential to propagate throughout the heart. For this reason, the cardiac muscle cells within the heart can be considered as a functional syncytium, electrical and mechanical, which allows a single action potential to pass through the heart causing it to contract properly [1].

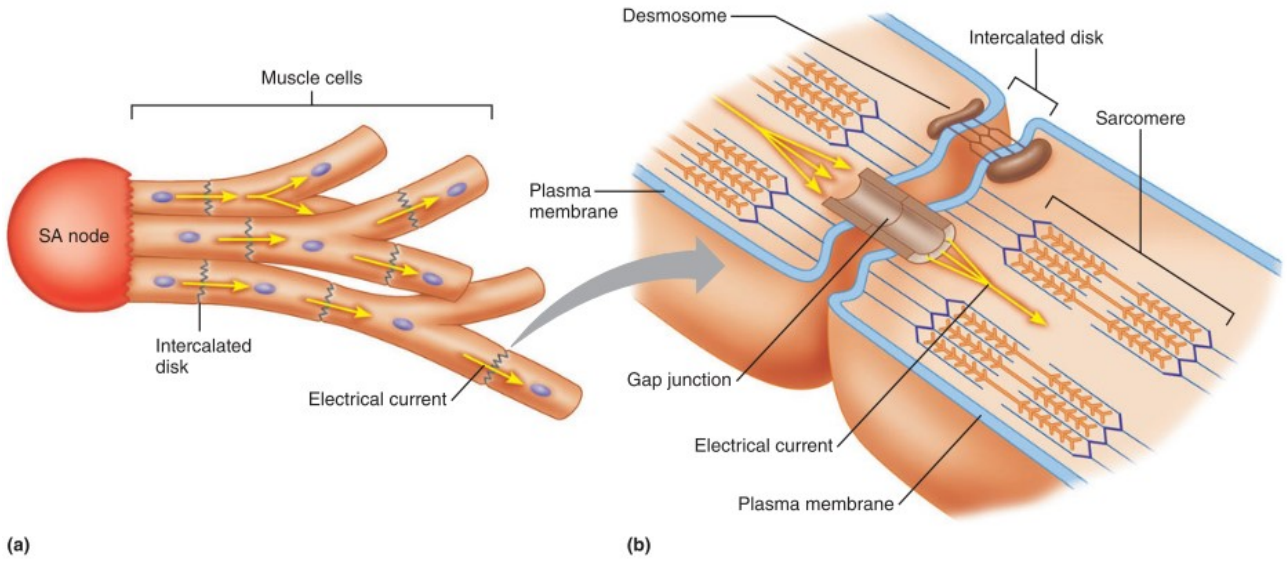

Figure 5: **Electrical connections between cardiac muscle cells. (a)** An action potential is spontaneously generated from the SA node which propagates to adjacent muscle cells through the gap junctions in intercalated discs. **(b)** Structure of the junction between two adjacent muscle cells [1].

Unlike skeletal muscle, the heart does not require any commands from the central nervous system, but the contractions are triggered by signals originating from within the muscle itself. Auto-rhythmicity is a characteristic of the heart that consists of generating its own rhythm on a periodic basis. This is due to the action of particular muscle cells, called autorhythmic cells, which generate little or no contractile force, and regulate the pumping action of the heart by providing and coordinating the rhythm to the heartbeat. Autorhythmic cells are divided into: *pacemaker cells*, which generate action potentials and impart heart rhythm, and *conduction fibers*, which transmit action potentials in a coordinated way. Together, they make up the conduction system of the heart.

1.3.2. THE PACEMAKER CELLS

The heart's contractions start from the pacemaker cells, which determine the rate or rhythm of the heartbeat by regularly generating action potentials. These particular cells originally seem to be muscle cells that have lost the contractile function but keep the ability to spontaneously depolarize and generate an electrical activity (action potential). Although are found in most of the heart, they are mainly concentrated in two specific regions of the myocardium: the *sinoatrial node* (SA node),

which is located in the wall of the right atrium near where it joins the superior vena cava and the *atrioventricular node* (AV node), located near the tricuspid valve in the interatrial septum [2].

Normally the action potential is generated when the electrical stimulus (electric current), coming from neighboring cells, is sufficient to depolarize the cell at the threshold. However, pacemaker cells, not having a constant resting potential like other cells, are able to generate action potentials without the need for external stimuli. At the end of an action potential, the membrane potential of the pacemaker cells is approximately -60 / -70 mV, and it slowly begins to depolarize until it reaches the threshold, thus creating a new action potential (*Figure 6*).

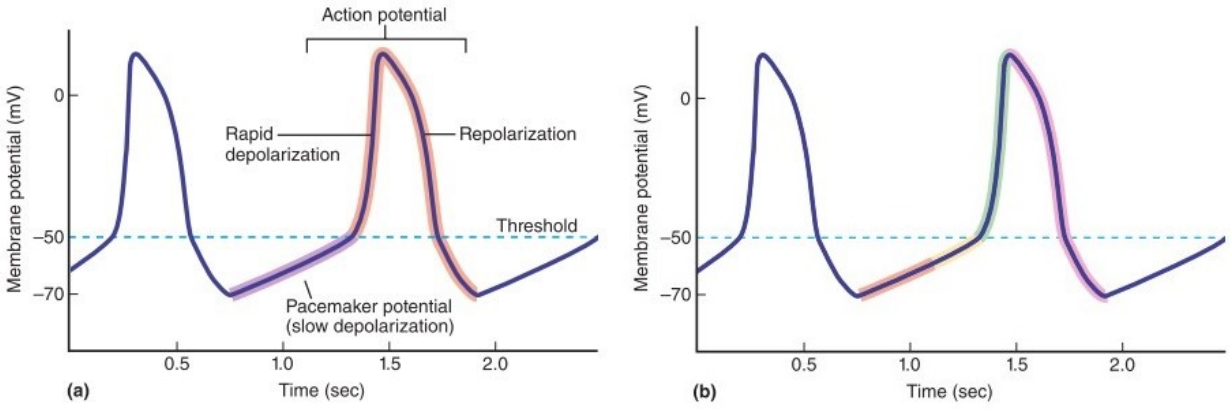

Figure 6: **Action potential of pacemaker cells. (a)** Form of action potentials of pacemakers. **(b)** Changes in membrane permeability during the generation of an action potential. Initially we have a slow spontaneous depolarization (orange), the potassium permeability decreases, and the sodium permeability increases. During the final depolarization (yellow), the calcium permeability increases, and the sodium permeability decreases. In rapid depolarization (green), the permeability of calcium increases. Finally, during repolarization (pink), the permeability of calcium decreases and the permeability of potassium increases [1]**.**

The depolarization or "ramp" phase that precedes the action potential is called the *pacemaker potential*. In pacemaker cells, as in other heart muscle cells, electrical signals are triggered by changes in the ionic permeability of the plasma membrane to sodium Na^+, potassium K^+ and calcium Ca^{2+} ions. The concentrations present in heart cells are characterized by an intracellular fluid rich in potassium, but poor in sodium and calcium compared to the extracellular fluid. The membrane potentials of the respective approximate ions are E_K = -94 mV, E_{Na} = +60 mV and E_{Ca} = +130 mV.) This means that an increase in permeability to sodium or calcium will make the membrane more positive, while greater permeability to potassium makes it more negative.

In the first phase of the potential, the closing of the potassium channels and the opening of the funny channels makes the movement of potassium out of the cell to decrease, while the movement of sodium inside the cell increases, causing the slow depolarization to take place. Funny channels open only for a short time and close when the membrane potential reaches 55 mV, so just before reaching the threshold where the action potential is generated. In the phase of repolarization of the action potential, on the other hand, the potassium channels open and then close again when the membrane returns to its initial state of polarization. The opening of voltage-gated calcium channels, called *T-type channels*, is triggered upon initial depolarization by increasing calcium permeability and consequently further depolarizing the cell. The T channels remain open for only a short time

and favor the opening of another type of voltage-gated calcium channels called *L-type channels*. Unlike the former, these remain open longer and close more slowly leading to a rapid depolarization. At this point the potassium channels open, which determine an increase in permeability and consequently a decrease in the membrane potential. Calcium channels are no longer stimulated and deactivate and begin to close. This is the repolarization phase in which the calcium flow inside the cell decreases and the potassium flow to the outside increases, ending the action potential [1].

1.3.3. THE NON-PACEMAKER CELLS

The action potentials of cardiac contractile cells are different from those of pacemaker cells. In particular, the action potentials coming from different areas of the heart vary according to the shape and speed of propagation. This is due to the fact that there are multiple types of contractile cells and they differ in the number of ion channels present. However, two important events characterize most cardiac action potentials: The first is that during the cardiac action potential, potassium permeability decreases as voltage-gated potassium channels close in response to depolarization (in pacemaker cells conversely, they open in response to depolarization); The second is that during a cardiac action potential action, depolarization causes tension-dependent calcium channels to open, affecting membrane potential and causing muscle cell contraction.

Furthermore, unlike pacemaker cells, contractile cells are characterized by a stable resting potential. The action potential itself has a different shape and can be divided into five phases (0 to 4), as shown in *Figure 7*:

- *Phase 0.* Phase 0 of the cardiac action potential is similar to the increase in a neuronal action potential. The initial depolarization of the membrane promotes the opening of the voltage-gated sodium channels, increasing the flow of sodium within the cell. The membrane potential becomes more positive and opens even more sodium channels, the permeability continues to increase, and the cell becomes more and more depolarized. The result is a rapid increase in the membrane potential up to values between +30 and +40 mV.
- *Phase 1.* Sodium channels that were opened in phase 0 begin to become inactivated and the sodium permeability decreases. The reduction in sodium flux causes the membrane potential to drop towards more negative values, as potassium ions simultaneously exit the cell. However, the potential reduction is small as membrane depolarization initiated in phase 0 has favored two other events: the closure of voltage-gated potassium channels, which reduce the flow of potassium out of the cell; and the opening of L-type calcium channels, which increases the flow of calcium into the cell. Both of these changes act to depolarize the membrane, thereby counteracting the sodium channel inactivation effect.
- *Phase 2.* During phase 2, also called the plateau phase, most of the potassium channels that were closed in phase 1 remain closed, causing the potassium permeability to remain below its resting value. At the same time, most of the calcium channels that opened in phase 1 remain open and the calcium permeability remains high. These two events keep the membrane in its depolarized state.
- *Phase 3.* During phase 3, the permeability of potassium increases due to the action of a second group of potassium channels (called delayed rectifier channels), which open in response to depolarization. These channels begin to open during phases 1 and 2, but their action does not greatly affect the membrane potential until phase 3 as they open slowly. As

the flow of potassium out of the cell increases, the membrane potential drops to more negative values. Furthermore, this drop in potential removes the stimulus that has kept the internal rectifier channels closed in phase 2 as they begin to open and will further increase the potassium flow. The drop in potential also removes the stimulus that kept the calcium channels open during phase 2 and allows them to start closing, reducing the flow of calcium into the cell. This phenomenon together with the increase in potassium flux repolarize the membrane, thus ending the action potential.

- *Phase 4.* During this phase, which corresponds to the resting potential, the various permeabilities of potassium, sodium and calcium are at the resting values. The membrane potential is approximately -90 mV [1].

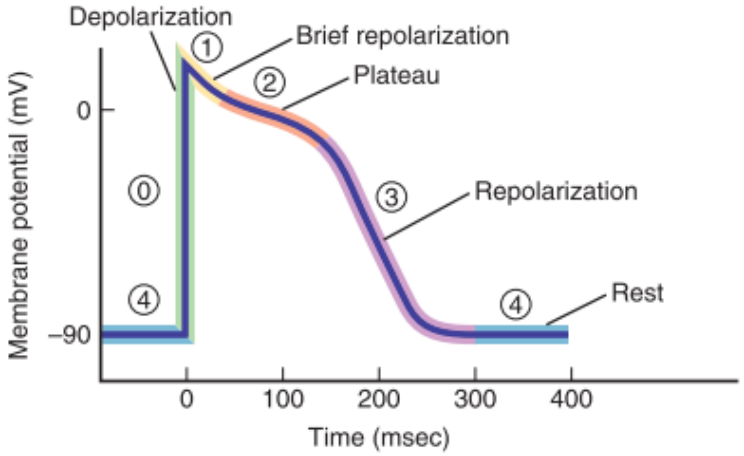

Figure 7: **Action potential of cardiac contractile cells.** During phase 0 (green) the permeability of the sodium increases and that decreases during phase 1 (yellow). During phase 2 (orange) the permeability of calcium increases and the permeability of potassium. Instead, in phase 3 (purple) the permeability of calcium decreases and permeability of potassium increases. During phase 4 (blue), all ion channels are in their resting state [1].

1.3.4. CONDUCTION OF THE IMPULSE DURING A HEARTBEAT

The initiation and conduction of the electrical impulse during the heartbeat follow a precise path (*Figure 8*):

1. The action potential is initiated in the SA node, from which travels to the AV node. The cells of the SA node can communicate with the cells of AV node through *internodal fibers*, systems of conduction fibers that run through the walls of the atria. Moving through the internodal pathways the impulse also spread through the atrial muscle by way of interatrial pathways.
2. The AV node transmits action potentials less rapidly than other cells of the conduction system resulting in a delay of about 0.1 second (AV nodal delay).
3. The impulse then travels through the atrioventricular bundle, also called bundle of His, which is a compact bundle of muscle fibers located in the interventricular septum. The AV node and bundle of His are the only electrical connection between the atria and the ventricles, which are otherwise separated by the fibrous skeleton.
4. The bundle of His splits into left and right bundle branches, conducting impulses to the left and right ventricles, respectively.

5. From the bundle branches, signals travel through an extensive network of branches called Purkinje fibers, which spread through the ventricular myocardium from the apex upward toward the valves. From these fibers, impulses travel through the rest of the myocardial cells.

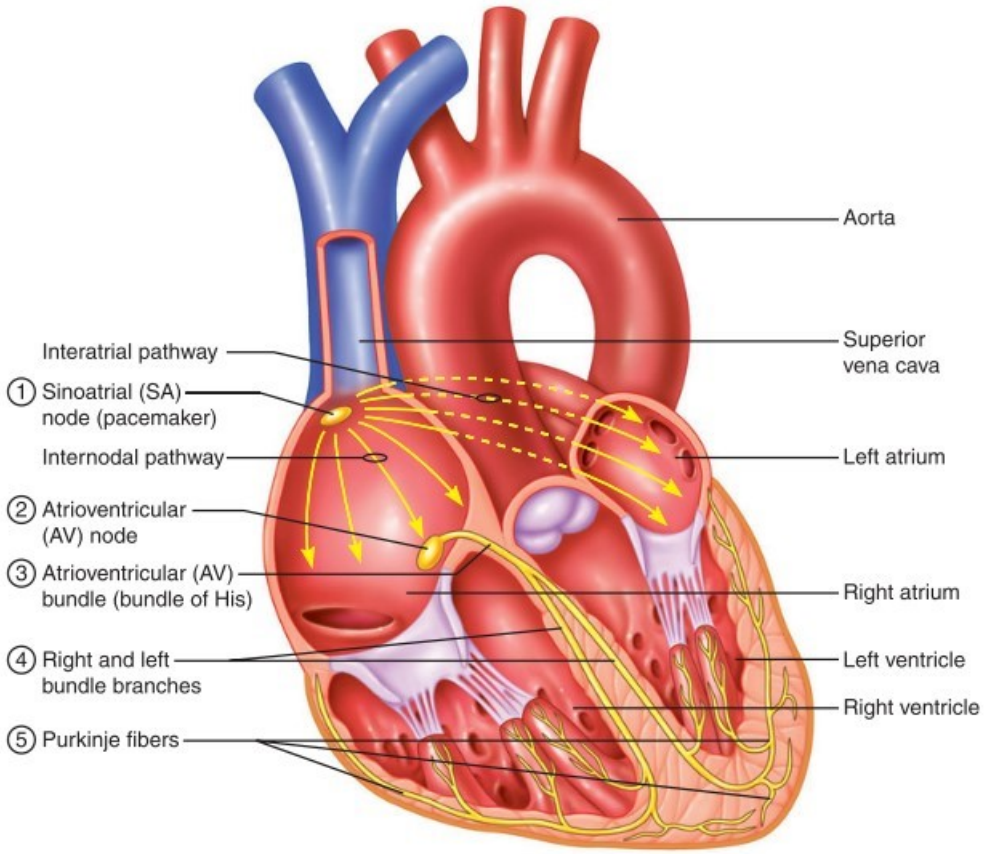

Figure 8: **Conduction system of the heart** [1].

Normally the heartbeat is triggered by electrical impulses originating from the SA node. When the action potentials travel through the AV node, cells go into a refractory period, during which no action potentials can arise. Moreover, the SA node is characterized by a higher frequency of action potentials, about 70 bpm, compared to 50 bpm for the AV node, making it rarely activate an action potential. The AV node is able to generate impulses when the SA node fails to fire or if it slows down dramatically, allowing normal ventricular contraction. It can also take control of the heartbeat if there is a block or slowdown in conduction between nodes.

1.3.5. THE ELECTROCARDIOGRAM

Electrocardiogram (ECG) is a non-invasive method of monitoring the electrical activity of the heart that causes the heart muscle to contract. ECG recordings are very important for doctors to determine if there are any problems or irregularities in the patient's heartbeat.

The ECG is a record of the overall spread of electrical current through the heart as a function of time during the cardiac cycle. Action potentials generated in individual myocardial cells cause currents to be conducted through the body fluids around the heart. The more synchronized the activity, the greater the amplitude of the signals that are recorded at a distance from the source. For this reason,

the recordings, which correspond to the various electrical phases of cardiac activity, can be made thanks to electrodes placed in certain positions on the patient's skin surface [3].

The standard ECG recording procedure is based on an imaginary equilateral triangle, called Einthoven's triangle, built around the heart and expanded to the upper and lower limbs as shown in *Figure 9*.

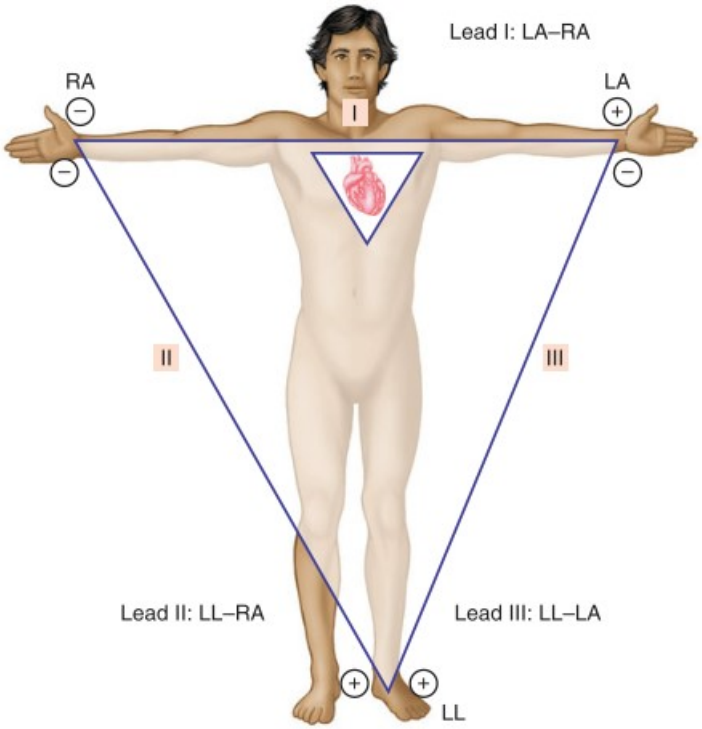

Figure 9: **Einthoven's triangle** [1]**.**

The electrodes are connected in pairs, positive and negative, to a voltage measuring device such as an oscilloscope which detects the difference of on the surface electrical potential. Each pair is renamed Leads and is indicated with Roman numerals. Lead I senses left arm potential minus right arm potential; Lead II detects the potential in the left leg minus that in the right arm; Lead III senses the potential in the left leg minus the left arm.

Chest or limb electrodes connected to 12 different cables can be used for ECG recordings. Each cable allows to acquire a different electrical image of the heart, thus obtaining different views for each recorded wave. The ECG, recorded on graph paper, shows three waveforms characteristic of our cardiac cycle (*Figure 10*):

- The P wave, is an upward deflection due to atrial depolarization;
- The QRS complex, is a series of deflections due to ventricular depolarization (correlates with phase 0 of the action potential of ventricular contractile cells);
- The T wave is an upward deflection caused by ventricular repolarization (related to phase 3 action potential of ventricular contractile cells).

Atrial repolarization is generally not detected in an ECG recording because it occurs simultaneously with the QRS complex.

In addition to waves, certain intervals and segments can provide important information about the heart's function. The P-Q or P-R interval occurs between the start of the P wave and the beginning of the QRS complex and is an estimate of the conduction time through the AV node. The Q-T interval is the time from the beginning of the QRS complex to the end of the T wave and is an estimate of the time the ventricles contract, called ventricular systole. The T-Q segment is the time between the end of the T wave and the beginning of the QRS complex and is an estimate of the time the ventricles relax, called the ventricular diastole. The R-R interval is the time between the peaks of two successive QRS complexes; it represents the time between heartbeats [1].

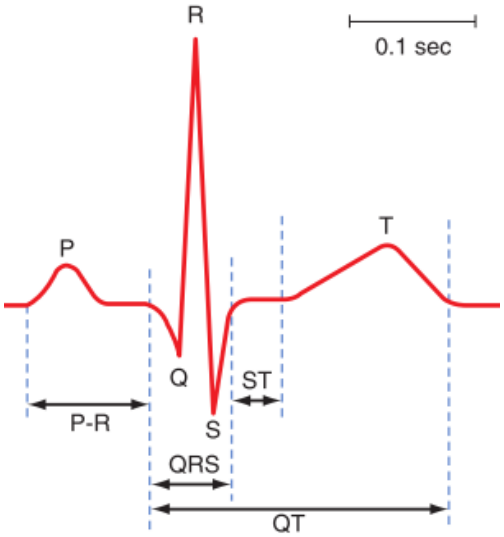

Figure 10: **Electrical activity of the heart.** Main characteristic waveforms and segments visible from ECG recordings are represented [1].

1.4. ARRHYTHMIAS

Cardiac arrhythmias belong to the cardiac pathology and are disturbances in impulse formation, in pacemaking or in conduction. Their effects can be neglectable, several people are even not aware that they have it, or very dangerous, if not treated immediately they could lead to death.

In the context of electrogenesis arrhythmias can be divided in: *abnormal impulse formation* and *abnormal conduction*. Abnormal impulse formation mechanisms in turn comprise two classes, both based on afterdepolarization: enhanced automatism and trigged automatism.

Automatism is the property of cardiac cells to undergo a spontaneous diastolic depolarization, and to initiate an electrical impulse in the absence of external electrical stimulation.

The *enhanced automatism* occurs only when the cells show alterations in their transmembrane potential, in particular during the resting phase, when these cells should be refractory to new depolarizations. This type of automatism can be achieved in three ways:

- Instability and increased slope (towards more positive values) of the membrane potential during the resting phase (phase 4);
- Shift of the maximum level of diastolic polarization towards less negative values;
- Shift of the potential threshold towards more negative values;

The slope of the repolarization curve can be more or less steep if in the presence of a different ionic composition of the extracellular fluid, of certain substances in circulation or of stimulation of the autonomic nervous system. The increased automatism can give rise to ectopic beats or be the trigger for tachyarrhythmias when the discharge activity of subsidiary pacemakers is such as to take sinus control of the heart rhythm [5].

The *triggered automatism* is initiated by afterdepolarization, defined as depolarizing oscillations in the membrane voltage that follow one or more previous action potentials. Unlike enhanced automatism, triggered automatism is not a self-generated rhythm but, arises as a response to an impulse (trigger). An automatic rhythm, on the other hand, can arise de novo in the absence of a previous potential. Afterdepolarization is defined *early afterdepolarization* when occur during the repolarization phase (EAD, phase 2-3 of the action potential) or *delayed afterdepolarization* if occur after the completion of repolarization (DAD, phase 4). Not all afterdepolarizations reach the potential threshold, but when they do, a new action potential is generated.

Reentry is the most common mechanism underlying arrhythmias due to abnormal conduction. The reentry mechanism occurs when an excitation wave is not extinguished following a normal cardiac activation but activate again the cardiac tissue. Under normal conditions, the depolarization waves spontaneously extinguish following the complete activation of the cardiac tissue due to the phenomenon of refractoriness. In this condition the cells are prevented from being re-excited for a period proportional to the duration of the action potential. In pathological conditions, some excitation waves can become blocked in crossing limited areas, rotate around the same areas and return to the starting site in repetitive cycles. These depolarization waves, deviating from the normal activation circuit, are not extinguished because at the exit of the pathological circuit they encounter excitable myocardium which is no longer in refractory period.

Cardiac arrhythmias can be classified into bradycardia (situation in which the heart goes slower than normal) and tachycardia (situation in which the heart goes faster than normal). The difference between the various types of arrhythmia depends on which parts of the heart it originates and which parts it crosses:

- *Supraventricular arrhythmias*: originates in the atria ("Supra" means above; "ventricular" refers to the lower chambers of the heart, the ventricles);
- *Ventricular arrhythmias*: Arrhythmias that begin in the ventricles;
- *Bradyarrhythmias*: Slow heart rhythms that may be caused by disease in the heart's conduction system, such as the sinoatrial (SA) node, atrioventricular (AV) node or HIS-Purkinje network.

Types of supraventricular arrhythmias include:

- *Premature atrial contractions (PACs)*: Early, extra heartbeats that originate in the atria;
- *Paroxysmal supraventricular tachycardia (PSVT)*: A rapid but regular heart rhythm that comes from the atria. This type of arrhythmia begins and ends suddenly;
- *Accessory pathway tachycardias (bypass tract tachycardias)*: A fast heart rhythm caused by an extra, abnormal electrical pathway or connection between the atria and ventricles. The impulses travel through the extra pathways as well as the usual route. This allows the

impulses to travel around the heart very quickly, causing the heart to beat unusually fast (Wolff-Parkinson-White syndrome);

- *AV nodal re-entrant tachycardia (AVNRT)*: A fast heart rhythm caused by the presence of more than one pathway through the atrioventricular (AV) node;
- *Atrial tachycardia*: A rapid heart rhythm that originates in the atria;
- *Atrial fibrillation*: Many impulses begin and spread through the atria, competing for a chance to travel through the AV node. The resulting rhythm is disorganized, rapid and irregular. Because the impulses are traveling through the atria in a disorderly fashion, there is a loss of coordinated atrial contraction;
- *Atrial flutter*: An atrial arrhythmia caused by one or more rapid circuits in the atrium. Atrial flutter is usually more organized and regular than atrial fibrillation.

Types of ventricular arrhythmias include:

- *Premature ventricular contractions (PVCs)*: Early, extra heartbeats that originate in the ventricles. Most of the time, PVCs don't cause any symptoms or require treatment;
- *Ventricular tachycardia (V-tach)*: A rapid heartbeat that originates in the ventricles. The rapid rhythm keeps the heart from adequately filling with blood, and less blood is able to pump through the body. V-tach can be serious, especially in people with heart disease, and may be associated with more symptoms than other types of arrhythmia;
- *Ventricular fibrillation (V-fib)*: An erratic, disorganized firing of impulses from the ventricles. The ventricles quiver and cannot generate an effective contraction, which results in a lack of blood being delivered to the body. This is a medical emergency that must be treated with cardiopulmonary resuscitation (CPR) and defibrillation (delivery of an energy shock to the heart muscle to restore a normal rhythm) as soon as possible;
- *Long QT*: The QT interval is the area on the ECG that represents the time it takes for the heart muscle to contract and then recover, or for the electrical impulse to fire and then recharge. When the QT interval is longer than normal, it increases the risk for "torsade de pointes," a life-threatening form of ventricular tachycardia.

Types of bradyarrhythmias include:

- *Sinus node dysfunction*: Slow heart rhythms due to an abnormal SA node;
- *Heart block*: A delay or complete block of the electrical impulse as it travels from the sinus node to the ventricles. The level of the block or delay may occur in the AV node or His-Purkinje system. The heartbeat may be irregular and slow [1].

2. ATRIAL FIBRILLATION

Atrial fibrillation is one of the most common arrhythmias in the world that can lead to serious complications in affected individuals.

It is a supraventricular arrhythmia characterized by a rapid and irregular heart rhythm, due to the presence of multiple waves resulting from small chaotic re-entries that occur within the atria (*Figure 11*). The onset and maintenance of this type of disorder may be due to the activation of ectopic focuses in venous structures adjacent to the atrial chambers, such as the ostia of the pulmonary veins. In the presence of atrial fibrillation, the atria cannot contract properly, and the atrioventricular node is subject to multiple electrical stimuli that cause an irregular transmission of impulses to the ventricles. The result is therefore a reduced contractile capacity of the myocardium of the heart and a consequent difficulty in pumping blood throughout the body [6].

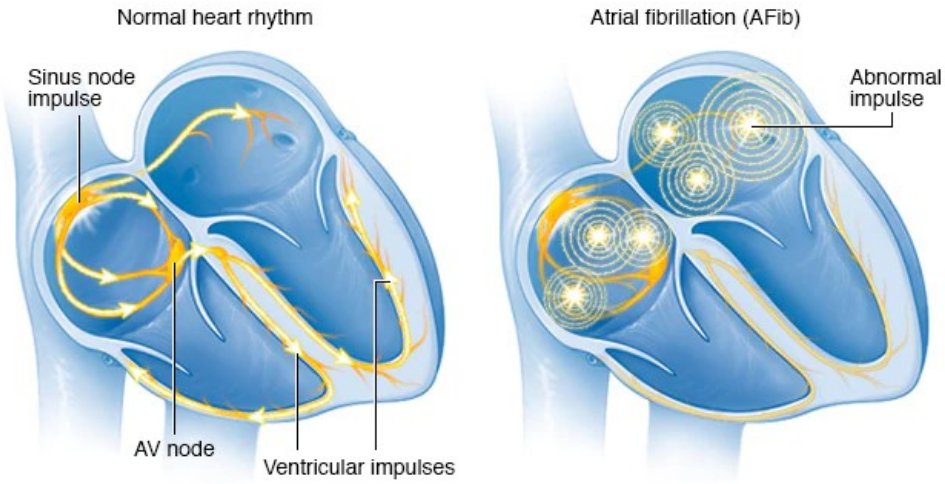

Figure 11: **Electrical impulses during atrial fibrillation.** On the left electrical conduction during normal heartbeat, on the right electrical conduction during atrial fibrillation [7].

Complications related to this type of arrhythmia, with consequent lack of atrial contraction, which can arise are the possibility of thrombus formation and therefore risk of stroke. The presence of blood clots can also lead to dysfunction or necrosis of limbs or organs. The absence of contraction of the atria can also alter the cardiac output, which will be decreased to a normal heart rate. This effect is usually well tolerated by the patient, with the exception of too high ventricular rate rhythms (for example> 140 bpm) or in situations where the range is already low from the beginning. In these situations, heart failure could occur.

Atrial fibrillation is the most common arrhythmia found in the clinic with a worldwide prevalence of 37,574 million cases, equal to 0.51% of the world population, which has grown by 33% in the last 20 years. The highest rate is found in countries with a high socio-demographic index, although the largest recent increase has been in countries with a medium socio-demographic index [8]. Atrial fibrillation mainly affects men and whites, compared to women and blacks. The incidence is also closely linked to age, with a prevalence ranging between 0.4% and 1% in the general population and which increases exponentially. Starting from the age of 50, the prevalence of AF doubles for each subsequent decade of life: from 0.5% in the decade between 50 and 59 years, it passes to 5-7% in the decade between 70 and 79 years, to pass finally to 8-10% in the age group > 80 years [5].

2.1. ETIOLOGY

The most common causes of atrial fibrillation are:

- Hypertension: is sustained elevation of resting systolic blood pressure (≥ 130 mm Hg), diastolic blood pressure (≥ 80 mm Hg), or both;
- Coronary artery disease (CAD): involves impairment of blood flow through the coronary arteries, most commonly by atheromas;
- Cardiomyopathy: is a primary disease of the heart muscle that usually manifests as heart failure and varies depending on whether there is systolic, diastolic, or both dysfunction;
- Mitral or tricuspid valvopathies: is any cardiovascular disease process involving one or more valves of the heart and result in diminished heart functionality depending on the type and severity of the disease;
- Hyperthyroidism: is characterized by hypermetabolism and elevated serum levels of free thyroid hormones;
- Alcohol abuse

Less frequent causes are instead linked to: Pulmonary embolism, atrial septal defects and other congenital heart defects, Chronic Obstructive Pulmonary Disease, Myocarditis and Pericarditis. Finally, isolated atrial fibrillation is the one without any identifiable cause that occurs in patients aged <60 years.

2.2. CLASSIFICATION

From a clinical point of view, atrial fibrillation is divided according to the mode of presentation into:

- Paroxysmal atrial fibrillation: characterized by a duration typically < 48 hours and which spontaneously converts to sinus rhythm (events may occur with repetition);
- Persistent atrial fibrillation: characterized by a duration > 1 week and requires intervention to be stopped;
- Long-lasting persistent atrial fibrillation: lasts > 1 year, but there is still the possibility to restore sinus rhythm;
- Permanent atrial fibrillation: characterized by a longer duration of atrial fibrillation, spontaneous conversion to sinus rhythm is less likely and its cardioversion is more difficult due to atrial remodeling (change in atrial electrophysiology due to high activation rates, such as reduced atrial refractoriness, increased spatial dispersion of the atrial refractory and/or decrease in intra-atrial conduction velocity);

The persistent and permanent forms are clinically more severe than the paroxysmal one [].

2.3. SYMPTOMS

Patients with atrial fibrillation are often asymptomatic and are diagnosed following cardiac examinations. In this case, if there is no alarm signal, there is a risk of a delay in treatment. There may therefore be a reduction in functional capacity and an increased risk of embolisms.

The main symptoms that are felt in the presence of atrial fibrillation are palpitations, vague chest discomfort, dizziness, fainting or symptoms of heart failure, such as weakness or shortness of breath.

An irregular pulse may also be present. Patients may also have symptoms and signs of acute stroke or damage to other organs due to embolisms. Symptoms can be episodic or quite frequent, especially during physical exertion and depend a lot on the patient's clinical condition (e.g. presence of hypertension, diabetes, heart failure).

2.4. DIAGNOSIS

Atrial fibrillations start by an ectopic beat arising close to the opening of the pulmonary vein in the left ventricles. It Is characterized by irregular baseline due to small re-entry circuits. The diagnosis of atrial fibrillation is performed through an arrhythmological examination from the analysis of the ECG traces (*Figure 12*) that will present:

- Absence of P waves related to atrial depolarization
- Presence of f (fibrillatory) waves between QRS complexes; f waves are irregular in frequency and morphology, characterized by a frequency> 300 ms (usually better visible in lead V1) and usually observable in the frequency band between 4-10 Hz
- Irregular R-R intervals

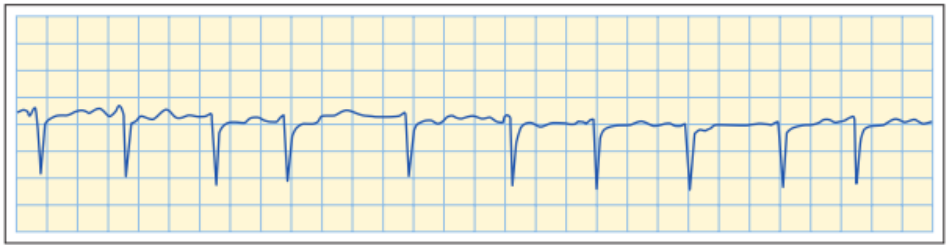

Figure 12: **ECG recording of atrial fibrillation** [2]**.**

Echocardiography and the thyroid function test are also essential tests in the initial evaluation. In particular, the echocardiogram is important for assessing the presence of structural heart disease, such as atrial enlargement, valvular heart disease, cardiomyopathy) and for the identification of additional stroke risk factors. Regarding the thyroid function test it is important as it performs the function of making hormones that affect the regulation of the heartbeat [5].

2.5. TREATMENT

The choice of therapy is made in relation to the form of atrial fibrillation, the presence of heart disease, symptoms and recurrence of the problem. The main strategies are:

- VENTRICULAR FREQUENCY CONTROL
- RHYTHM CONTROL
- ABLATION PROCEDURES FOR ATRIAL FIBRILLATION

2.5.1. VENTRICULAR FREQUENCY CONTROL

For patients with atrial fibrillation, regardless of duration, it is important that the resting heart rate is < 100 bpm) in order to control symptoms and prevent cardiomyopathies due to tachycardia. In particular, drugs are used such as blockers of the atrioventricular node in the presence of acute high-frequency paroxysms, beta-blockers in the presence of excess catecholamines (due to thyroid disorders or induced by exercise) or calcium antagonists.

2.5.2. RHYTHM CONTROL

In patients with heart failure or with evident hemodynamic impairment, sinus rhythm is restored to improve cardiac output. In other cases, conversion of atrial fibrillation to sinus rhythm is indicated, taking into account the fact that commonly used antiarrhythmic drugs can have adverse effects. Conversion to sinus rhythm does not eliminate the need for chronic anticoagulation.

Synchronized electrical cardioversion or medication can be used. If the atrial fibrillation lasts > 48 h, an oral anticoagulant is usually also prescribed to reduce the risk of ischemic stroke. Synchronized electrical cardioversion is carried out by supplying direct current (biphasic defibrillator set at 100 joules, followed by 200 and 360 joules), allowing a reset of cardiac activity and then conversion to sinus rhythm. It is usually more effective in the presence of atrial fibrillation of shorter duration, isolated or if induced by a reversible cause.

As for the use of drugs, on the other hand, class Ia, Ic, III antiarrhythmics are usually indicated, whose effectiveness is around 50-60% of patients (side effects vary according to the type of drug). Drugs used for rhythm conversion are also used for long-term maintenance of sinus rhythm.

2.5.3. ABLATION

In patients in whom it is not possible to use drugs for rhythm control, catheter ablation is indicated to correct atrial fibrillation. It consists of a minimally invasive procedure capable of treating atrial fibrillation or reducing the number of episodes by isolating (ablating) the abnormal electrical pathways present in the heart tissues. In order to obtain maximum effectiveness from the procedure, it is very important to select the patient to undergo ablation, as there is still the possibility of non-negligible complications. Once the symptoms presented by the subject have been analyzed, the type of atrial fibrillation, the presence of related heart disease, the intake of rhythm control drugs and therefore whether the patient has previously undergone drug therapies will be considered [10].

Catheter ablation is usually indicated in symptomatic patients with paroxysmal or persistent atrial fibrillation after the failure of an antiarrhythmic (class I or III) or as "first line therapy" in symptomatic patients with paroxysmal atrial fibrillation.

A greater probability of success was found in patients with paroxysmal atrial fibrillation, aged <60 years and in the absence of structural heart disease and with normal left atrium size. In particular, it is also indicated as first-line therapy, as an early rhythm control therapeutic approach, especially in young people, allows better results in reducing long-term relapses.

In the presence of persistent forms of atrial fibrillation lasting> 1 year, it has been shown to be less effective as a therapy. This is due to the fact that in the persistent form there is an electrical and structural remodeling at the atrial level which modifies the arrhythmic substrate making it more resistant to ablation. Even worse outcomes occur in older, hypertensive patients with obesity, with significantly dilated left atrium and presence of fibrosis on Nuclear Magnetic Resonance.

Finally, the decision to proceed with ablation can also be considered in patients with aggravated heart failure or caused by the atrial fibrillation itself. In these cases, the invasive procedure is carried out after having restored the sinus rhythm through electrical cardioversion, in the case of persistent forms, or after having made an attempt to control the rhythm with antiarrhythmic drugs [9].

3. ABLATION FOR ATRIAL FIBRILLATION

Catheter ablation is a minimally invasive procedure that works by using energy to heal or destroy a small area of heart tissue to prevent abnormal electrical signals from spreading through the heart. It is used to resolve certain types of arrhythmias or irregular heartbeats where drug treatment has not been possible or has not been successful.

Example of application of this procedure is atrial fibrillation. It consists in the electrical isolation of the sites of onset of this arrhythmia, normally recognized in the pulmonary veins, on which it acts preferentially at the antral level. However, the effectiveness of this procedure decreases in persistent atrial fibrillation, particularly in long-lasting atrial fibrillation as it is prone to substrate alterations, such as dilation and left atrial fibrosis. In these situations, a lesion is created at the level of complex fractional atrial electrograms (CFAE) and/or linear lesions at the level of the mitral isthmus, the posterior wall and the roof of the left atrium. Obviously, the atrial damage will be greater and there will be a greater risk of complications such as cardiac perforation or pro-arrhythmia (atrial flutter and macroriental atrial tachycardias) [12].

3.1. PROCEDURE

Catheter ablation is a relatively invasive procedure that is performed in a hospital electrophysiology laboratory (*Figure 13*) by experienced staff. The chamber must be equipped with:

Figure 13: **Electrophysiology lab suite** [11]**.**

- Radiolucent couch;
- X-ray equipment;
- Polygraph;
- Surgical set for the implantation of an implantable cardioverter pacemaker or defibrillator and for isolation of the pulmonary vein;
- Stimulator for Electrophysiology;
- Instrumentation for electrocoagulation;
- Programmers for implantable pacemakers and cardioverter defibrillators;
- Supply of material for maintaining sterility;

- Apparatus for general anesthesia;
- Automatic ventilator with complete set for resuscitation;
- Complete set for pericardiocentesis;
- Mapping system;
- Device for the delivery of radiofrequency;
- Cardiac imaging diagnostics (transesophageal echocardiography, CT or MRI);
- Tran septal puncture kit [13].

It is necessary to stop taking antiarrhythmic drugs five half-lives before treatment. Before the procedure begins, the patient will be given intravenous medications to help relax and even fall asleep, as it involves considerable psycho-physical stress since he will have to remain motionless for a few hours on the operating table.

The procedure consists of placing ablation and diagnostic catheters inside the heart chambers, which can be used for both sensing and pacing. Using a short, hollow tube, called catheter sheath, several flexible catheters are advanced into the patient's blood vessels, usually the femoral vein, internal jugular vein, or subclavian vein as shown in *Figure 14*, and then access the atrial cavities through the inferior (or superior) vena cava. One of the leads will be positioned at the apex of the right ventricle allowing stimulation if necessary.

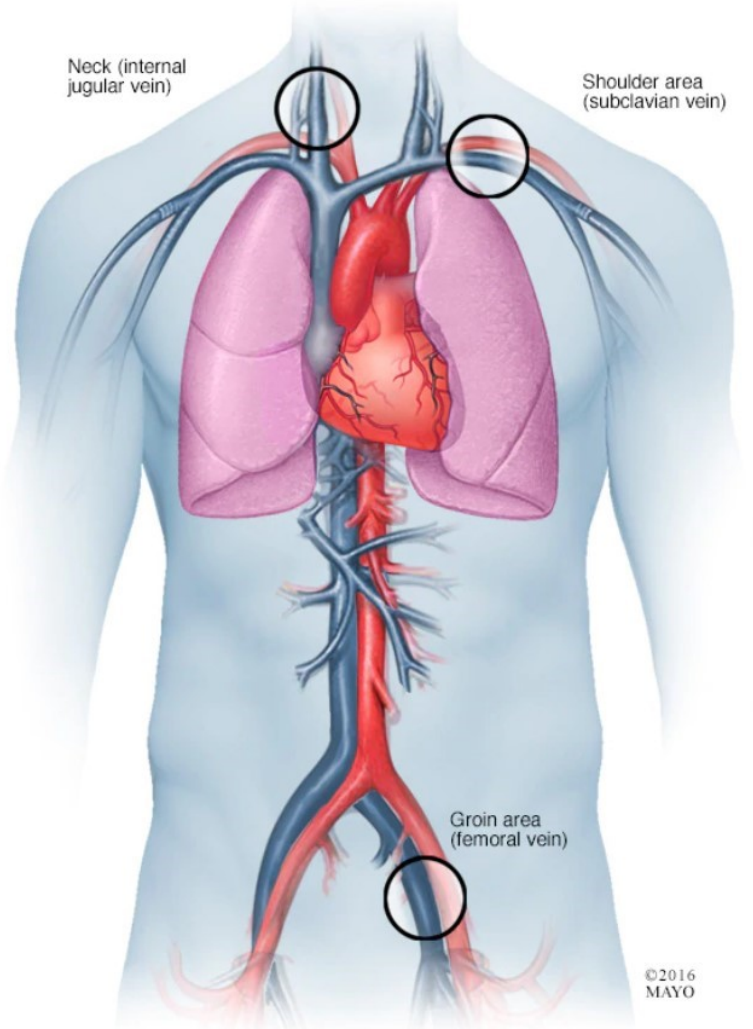

Figure 14: **Catheter access points for cardiac ablation** [7]**.**

Once the catheter reaches the heart, the doctor guide it to the area causing the arrhythmia. Modern 3D mapping systems are used to reconstruct the atrial geometry, to which will be added a voltage map and a map of activation delays, displayed using a color code. Voltage Map constitutes a map of the amplitude of the signals and therefore on the voltage of the electrograms and allows to distinguish the normal areas from those with low voltage (less than 1.5 mV). The activation map, on the other hand, represents the activation zones of the atrium, allowing the display of the dynamics of the arrhythmia. These maps are reconstructed starting from the signals recorded by diagnostic catheters (sensing), also allowing a precise localization of the scaler catheter and of the areas of interest to be ablated. The task of the biomedical engineer, on the recommendation of the doctor, is to highlight on the map the anatomical sites of main interest, such as the His bundle or the coronary sinus, as reference points to avoid unnecessary injuries. To accurately identify the areas of origin of the arrhythmia, the doctor stimulates the patient's heart itself and then proceeds with targeted lesions. Through specific targets the areas just treated will be highlighted during the procedure in order to keep track of the lesions. Both the electroanatomical map and the ECG tracings will be used to verify the effectiveness of the procedure [14].

For arrhythmias with an apparent focal origin (automatism and micro-orientations), the goal of ablation is the focus itself. In macrooriental tachycardias there is typically the presence of inexcitable scar tissue that separates the normally functioning myocardial flaps, therefore the goal of ablation is precisely the residual myocardium.

The total duration of the procedure can vary from 2 to 4 hours (depending on the arrhythmia to be treated), but in case of complications it takes longer. A short hospital stay is required for the procedure, typically 1-3 days. The patient is mobilized the day after ablation and a post-procedural echocardiogram is always performed before discharge, which occurs 24-36 hours after ablation (in the absence of complications) [15].

3.2. FOLLOW-UP

Following the surgery, the patient will have to remain under observation for 12-24 hours and will be constantly monitored by ECG. During the period just following the procedure, the risk of the arrhythmia recurring is greater, then decreasing over time. If there are no complications of any kind, after two days the patient is usually discharged and can resume daily activities. Functional recovery, on the other hand, takes about a week.

In the event that the patient, prior to ablation, was subjected to antiarrhythmic drug therapy, he must continue it. Only later, in the absence of relapses and under the indication of the treating doctor, can it be suspended. Anticoagulant therapy can instead be suspended 3 months after surgery and in the absence of reappearance of atrial fibrillation or risk of embolism.

Finally, there is a check by Holter ECG after one month, 6 months and 1 year from the procedure and an echocardiogram after 6 months from the procedure [16].

3.3. RISKS AND COMPLICATIONS

Although catheter ablation has proved to be a very effective treatment in resolving atrial fibrillations, it remains a complex procedure and therefore is not free from risks and complications. Their incidence varies in accordance with the extent of the lesions, the patient's characteristics, such as the presence of ischemic heart disease, heart failure, arterial or coagulopathies, and finally the

COMPLICATION	INCIDENCE (%)
Death	0.1
Cardiac tamponade	0.0-2.9
Thromboembolic events	0.0-1.1
Silent brain embolism	7-40.5
Pulmonary vein stenosis	0.0-0.5
Phrenic nerve paralysis	0.1-17
Atrioesophageal fistula	0.03-0.25
Periesophageal vagal damage	1
Vascular complications	0.2-2.5
Occlusion of the circumflex artery	0.002
Entrapment of the catheter in the mitral	0.01
Atypical atrial flutter / atrial tachycardia	3-40

Table 1: **Complications due to ablation of atrial fibrillation and its incidence** [9]**.**

experience of the Center. The complications that can occur are predominantly intraoperative and are listed in *Table 1*.

The most frequent are of the vascular type (0.2-2.5%) and consist of damage to the vessels in which the catheters are made to slide: hematoma, thrombophlebitis, deep vein thrombosis, arteriovenous fistula, arterial dissection. They are resolved with medical therapy and bed rest and only rarely require transfusions or surgery [9].

As for cardiac complications, they occur much more rarely. A recently recognized complication of catheter ablation of AF is silent brain embolism which appears to be related to the levels of anticoagulation during the procedure and is exponentially increased by electrical cardioversion. The clinical significance of post-ablation silent cerebral embolism, especially as a function of the possibility of developing cognitive decline and premature dementia, is unknown [17].

Other frequent complications related to ablation are stroke, pulmonary vein stenosis, phrenic nerve paralysis and local vascular lesions.

There are also risks due to transseptal punctures although, thanks also to the use of new sensors, they are less than 1%. Examples are accidental punctures of the posterior wall of the left atrium and accidental punctures of the main adjacent ones, such as the aorta, the consequences of which are very serious and potentially fatal and must therefore be promptly treated and resolved.

Another complication that must be taken into consideration is exposure to radiation that often results in skin burns and an increased risk (for both the patient and the doctor) of developing a long-term malignancy [18].

Regarding mortality related to catheter ablation of AF, the reported prevalence is approximately 1 per 1000 in 32569 patients undergoing 45115 procedures. Cardiac tamponade, a relatively frequent complication, shows the lowest mortality (2.3%), while atrioesophageal fistula, a rare complication, has a very high mortality (71%) [9].

3.4. CATHETERS

The term ablation indicates the removal of a body part or the destruction of its function. Catheter ablation is a minimally invasive ablative therapy, capable of treating malignant disorders such as atrial fibrillation. The procedure consists in introducing a small catheter or applicator into the body, aided by an image guidance system (e.g. CT, US, MRI) and once the target is located, energy is delivered to the tip of the applicator, and the applicator-tissue interface is treated [19].

Catheter ablation can be based on two different operating principles in relation to the type of abnormal heart rhythm to be treated (*Figure 15*):

- Radiofrequency ablation: uses thermal energy;
- Cryoablation: uses very cold temperatures.

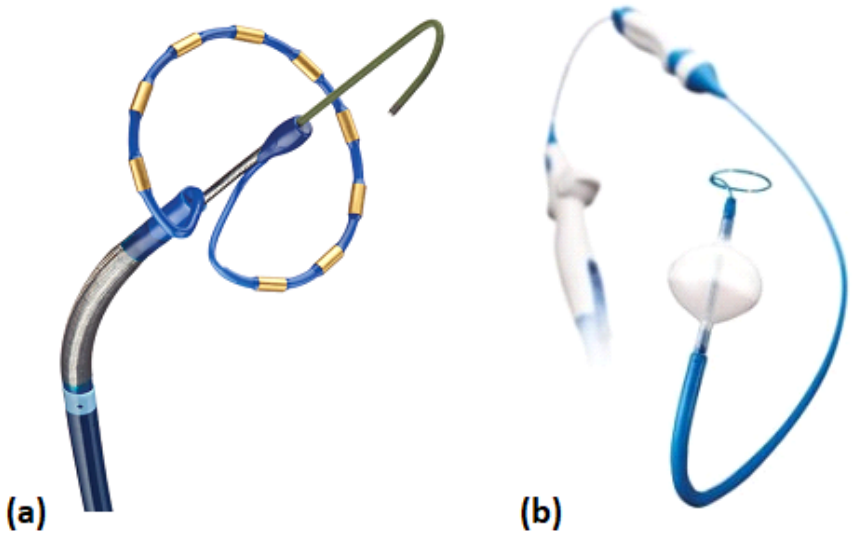

Figure 15: **Radiofrequency and cryoablation catheters. (a)** Pulmonary Vein Ablation Catheter GOLD (PVAC™ GOLD) produced by Medtronic; **(b)** Arctic Front™ Cardiac Cryoablation Catheter System produced by Medtronic [20-21].

3.4.1. RADIOFREQUENCY ABLATION

Radiofrequencies, electromagnetic waves generated by the alternating current emitted by an antenna, are the most used method for the ablation of arrhythmias. Radiofrequency technology does not provide deep lesions if compared to other techniques as laser or microwaves, which make radiofrequency ablation a preferential way for the treatment of cardiac tissues.

The instrumentation used for energy generation (*Figure 16*) does not require complex technology, and can be summarized conceptually as follows:

- Radiofrequency generator
- Radiofrequency catheter
- Reference patch electrode

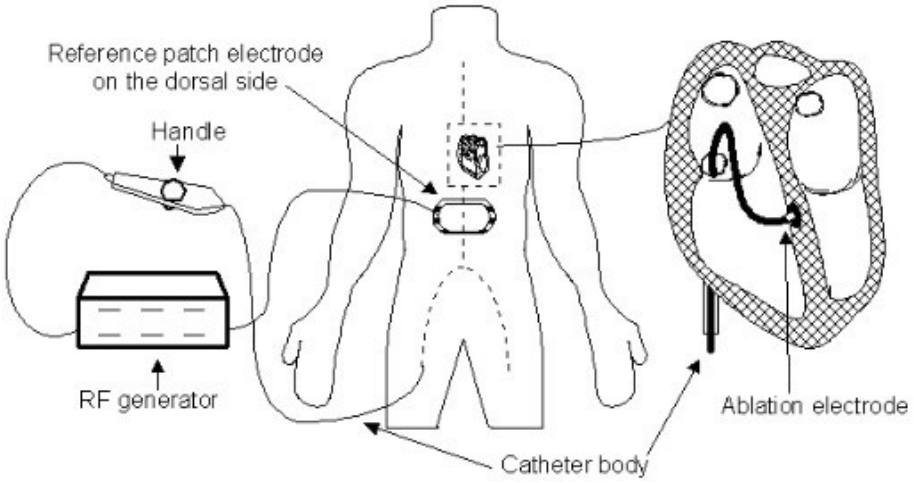

Figure 16: **Schematics of RF cardiac ablation system.** The RF catheter is inserted through the femoral vein and until it reaches the target site of the heart (right figure). A reference patch electrode (e.g. ground pad) is placed on the patient's back. The small black region around the RF electrode at the catheter tip depicts the ablation zone [22].

The radiofrequency energy supplied by a generator is conducted through cables to the tip of the catheter causing it to heat up and consequently also heating the tissue around the electrode itself. A ground pad placed on the patient's thighs or back acts as a return path for the radiofrequency current.

The energy is applied directly to the heart tissue, which having a high impedance determines the conversion of the energy delivered into heat (*Figure 17*). To have an irreversible lesion, it is necessary to reach a tissue temperature of 50 ° C. Temperatures above 90 ° C lead to the denaturation of blood proteins and to coagulation in contact with the electrode, creating a film of material that makes further energy supply impossible. The size of the lesion caused is closely linked to the time of energy application.

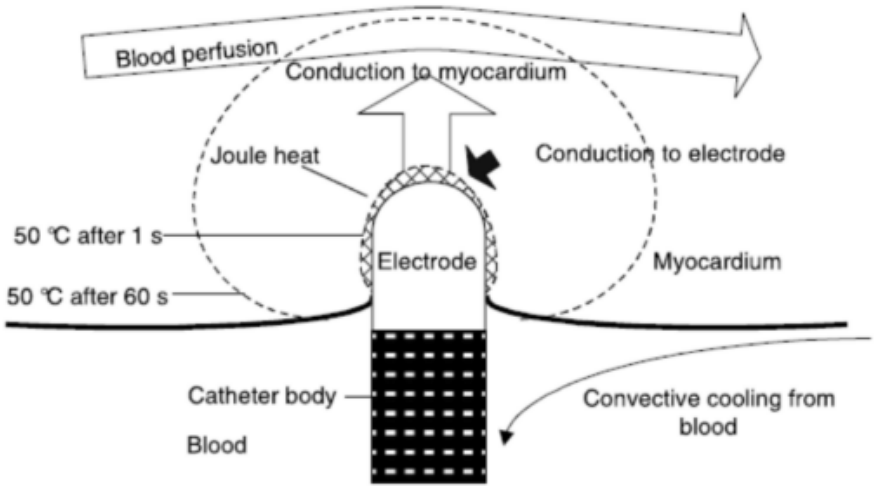

Figure 17: **Thermodynamics of cardiac RF ablation.** Thermal conduction of heat into the tissue results in growth of the ablation zone. Heat loss of tissue in proximity of the electrode due to thermal conduction through the electrode (black arrow); electrode and tissue surface experience convective cooling from blood inside the chamber (white arrow) [23].

Since the point of application is inside the body, the heat transfer and dissipation system are very complex and must also take into account the presence of blood circulating around it. In fact, blood perfusion works by locally cooling the electrode by removing a certain amount of heat by convection. It is therefore necessary for a correct ablation to find a balance between the heat that the catheter must provide and the convection effect [24].

This balance in term of temperature can be described thanks to the bio-heat *equation (1)*:

$$\rho c \frac{\partial T}{\partial t} = k \nabla^2 T + J \cdot E - \dot{Q}_h \qquad (1)$$

The term on the left side represents the change in tissue temperature due to radiofrequency heating. The first term on the right describes thermal conduction, which depends on the Laplacian of the temperature; the second term represents the heat generated by the radiofrequency current as the scalar product of the current density J produced under the radiofrequency field E; finally the third term $\dot{Q}_h$ refers to the heat lost by the blood perfusion. The latter is not known a priori but is modified according to the situation in order to better control (even automatically) the energy delivered by the radiofrequency electrode [25].

The blood perfusion can be viewed as a passive convection mechanism. Instead, an active convection mechanism can be used for cooling, consisting in the circulation of a convective fluid (typically water or saline infusion) within a system of lumens of the electrode. In relation to the structure of the catheter, the fluid can flow either inside it, and therefore will be called a closed circuit system, or through the openings of the electrode, and will instead be called an open irrigation system. A schematic representation of the two types is given in the *Figure 18*.

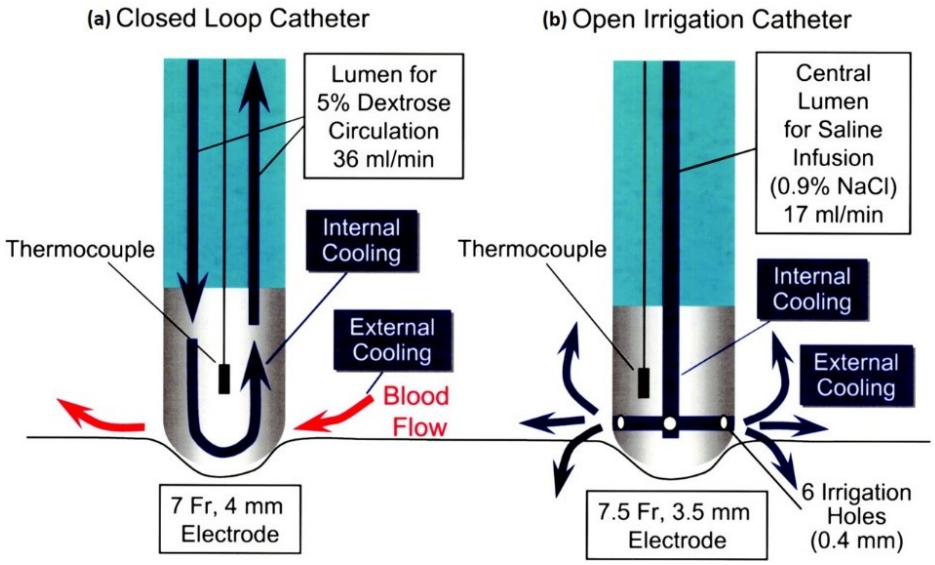

Figure 18: **Schematic representation of the irrigated electrode catheters. (a)** Closed loop irrigation catheter has 7F, 4-mm tip electrode with an internal thermocouple. A 5% dextrose solution at room temperature was circulated continuously through the tip electrode at a flow rate of 36 mL/min, cooling the ablation electrode internally. **(b)** Open irrigation catheter has 7.5F, 3.5-mm tip electrode with an internal thermocouple and 6 irrigation holes (0.4-mm diameter) located around the electrode, 1.0 mm from the tip. Saline infusion at room temperature was irrigated through the electrode and 6 irrigation holes at a flow rate of 17 mL/min, providing internal and external electrode cooling [26].

The fluid cools down both the electrode and tissue in close proximity, allowing the location of highest temperature move deeper into the tissue from the electrode surface. Cooling of the radiofrequency electrode is a commonly used method that allows to increase the ablation zone dimensions [27].

In absence of an active cooling system of the electrode, the highest temperature can be observed just near the electrode, decreasing as the distance increases as shown in the following graph (*Figure 19*):

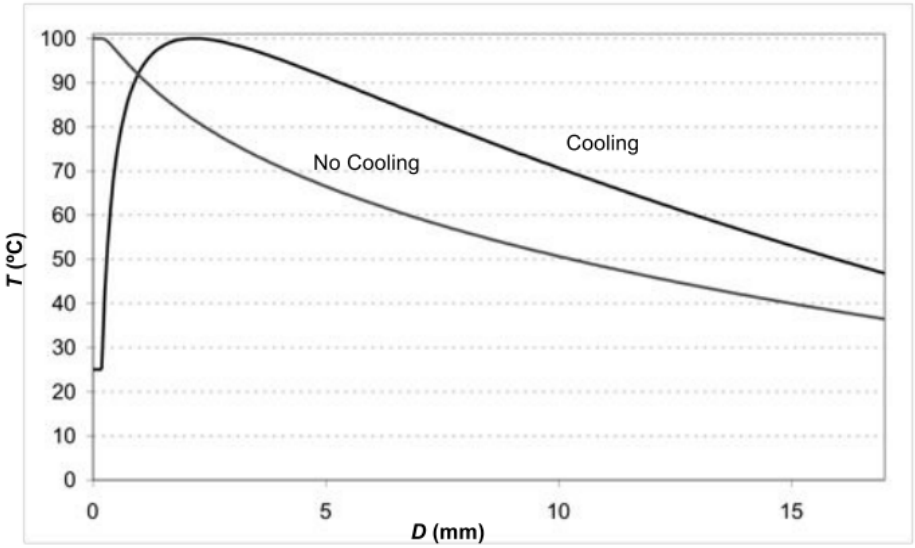

Figure 19: **Displacement of maximum tissue temperature relative to the ablation electrode.** (T) is the temperature and (D) is the distance. In the absence of cooling the maximum temperature is near the electrode, if a cooling system is applied, this position is moved away from the electrode, obtaining a larger ablation area [27].

Radiofrequency systems can be monopolar or bipolar. In unipolar systems, energy flows from the active electrode of the scaler catheter to the passive or dispersion electrode usually placed on the patient's back. When radiofrequency is delivered from the active electrode, current flows through the body and reaches the leakage electrode. The active electrode, having a very small area, has high current density values and therefore there is a high dispersion which causes an increase in the temperature of the surrounding tissue. Most of the absorption occurs in an area with a slightly larger radius than the electrode, so the interaction of the electromagnetic RF wave with the heart tissue results in a transformation of the wave into thermal energy. The passive electrode, on the other hand, having larger area, has a lower current density so that no heating of the tissue occurs.

In the bipolar system, on the other hand, the two active and passive electrodes are placed near the area to be ablated: this involves the passage of energy between small volumes of myocardium, allowing a more focused and uniform transmural lesion. The fact that the radiation passes through a very limited region means that the surrounding tissues do not heat up and therefore do not get damaged [28].

Each catheter has an ablation electrode and three recording electrodes that are able to detect the temperature and impedance of the system by sending this parameter to the console, which

regulates the amount of current delivered to the probe. In fact, during radiofrequency ablation there are several relevant parameters that must be monitored:

- *Power (Watt):* represents the emission power of radio waves and therefore the energy level contained within the radiation. The range normally used is variable between 5 Watts and 80-100 Watts depending on the characteristics of the generator and the scaler catheter. The power level must be chosen based on the anatomical position and depth of the desired ablation;
- *Temperature (°C):* the temperature reached by the catheter tip must be higher than the tissue temperature to induce lesions, but not excessively high in order not to induce charring and thrombus formation. The range is normally between 45 and 70 °C;
- *Duration (seconds):* usually, the minimum estimated duration considered effective is at least 15 seconds, while deliveries greater than 60 seconds are not considered effective in obtaining an extension of the lesion;
- *Impedance (ohm):* represents the ease with which radio frequencies pass through the circuit consisting of the tissues interposed between the tip of the catheter and the neutral electrode positioned at a point on the patient's skin. It is equal to the ratio between the voltage applied across the circuit and the intensity of the current flowing through it, so it does not require special sensors and can be measured by any catheter for ablation. Impedance monitoring, in addition to temperature measurement, is a useful method for measuring the power of the radio frequencies emitted. Given that the impedance progressively decreases as the tissues are altered by the passage of energy, an average reduction of 5-10 ohms is considered a sign of clinically effective ablation [29].

An innovation brought to the new ablation catheters is the introduction of a contact sensor capable of measuring the force and angle of application to the tissue. The force is measured in grams and represents a fundamental parameter both from a safety point of view, avoiding pressures that are dangerous for the integrity of the fabric, and for an evaluation of the effectiveness of delivery through direct contact. A stable force of 10 grams or more, for a period of at least 15 seconds, is considered effective for proper ablation.

3.4.2. CRYOABLATION

Cryoablation is a treatment that relies on cooling tissue to damage myocardial tissue and resolve the conduction of harmful electrical signals. It is able to reach temperatures below –20 ° C, at which point the water present in the intracellular fluid expands, freezing and causing the death of the cells of the affected tissue.

The size of the lesion created depends on several factors:

- Temperature
- Duration of freezing
- Freezing rate (how quickly the cryoprobe can lower the temperature, °C/s)
- Thawing rate (how quickly the temperature can return to room temperature, °C/s)

Each cryoablation system (*Figure 20*) consists of a cryoprobe and the console, which supplies the cryogen to the cryoprobe.

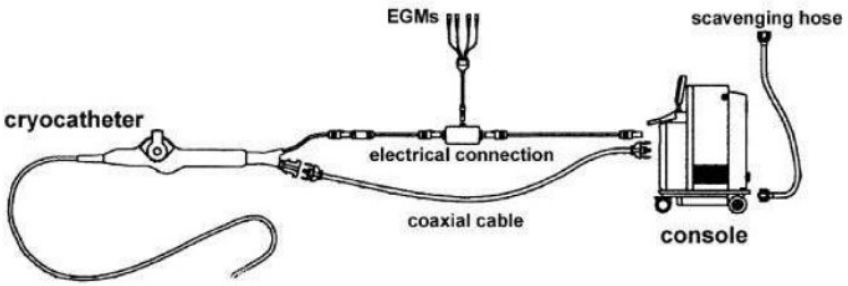

Figure 20: **Scheme of cryoablation system.** The steerable catheter and the console are connected by: a coaxial cable, used both to deliver fluid nitrous oxide to the catheter and to remove separately the gas from the catheter; electrical cable, which is connected both to the conventional recording system for electrograms (EGMs) analysis and storage and to the console for reading of the tip temperature. A tank of fluid nitrous oxide is located inside the console; the gas removed from the catheter to the console is evacuated through a scavenging hose into the vacuum line of the electrophysiology laboratory [30].

The console includes:

- Outlet for multiple probes
- A proper discharge system
- Sufficient source for liquid nitrogen
- Display and menu for controlling all the parameters (flowing rates, thawing rates, ablation durations)

The cryoprobes are needles in which gas or liquids at low temperatures circulate, housed in special catheters and connected to the console by means of special cables. The most used gases are carbon dioxide (CO_2), liquid nitrogen (LN_2), which is the most used due to its excellent refrigerating properties and ease of use, and liquid helium (LHe), which is instead very expensive and difficult to handle as it is volatile. In general, the working range is –60 to –80 ° C at the probe tip.

The LN_2 catheter consists of a closed-end tube with two tubes arranged concentrically within it (*Figure 21*). Inside, vacuum insulation must be guaranteed to avoid freezing up the shaft and subsequent destruction of normal tissue.

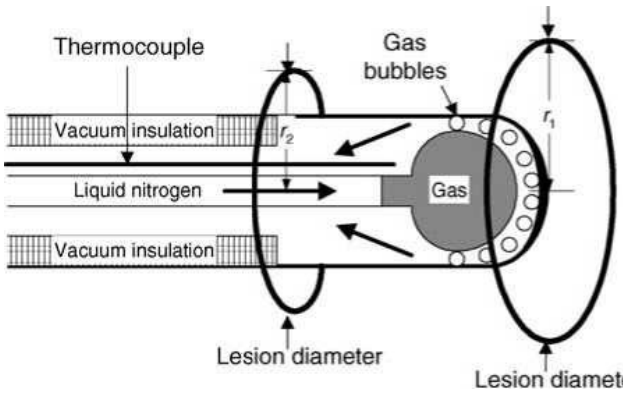

Figure 21: **Internal structure of a typical cryoprobe based on liquid nitrogen (LN_2).** The probe has vacuum insulation to prevent freezing of the probe shaft and subsequent destruction of normal tissue. The LN changes phase hitting the metal tip of the probe. A thin film of gas bubbles is formed on the metal surface resulting in lowest temperatures and largest ice ball near the tip.

The cryogen or liquid nitrogen is brought to the probe via an internal feed tube. As it flows towards the tip of the probe and hits the relatively hot metal of the probe, it changes the phase. A thin film of gas bubbles forms between the liquid and the metal, isolating the cryoprobe from the liquid. The flow of LN_2 at -206 ° C leaves the cryoprobe with a temperature below -196 ° C. Hence, the marked expansion in a gas is significantly reduced and a greater flow of cryogen is allowed in a smaller probe. The heat-extraction capability is 88 times better in LN_2 than in nitrogen gas. The correct functioning of the cryoprobe is monitored by means of a thermocouple. If the measured temperature is above -160 °C, the cryoprobe does not work properly and the procedure must be interrupted. This sensor also provides the information for a temperature feedback loop [31]. There are also other sensors for detecting the ECG signal for patient monitoring.

Therefore, thanks to the information detected by multiple sensors, the control console allows the surgeon to perform the ablation by modifying the parameters necessary to obtain a correct ablation.

4. MAPPING SYSTEM

Catheter ablation is a procedure that requires high precision and accuracy in creating lesions in specific regions of the heart chambers in order to electrically isolate them without the risk of causing pulmonary vein stenosis or perforations. For this reason, imaging systems are used that make it possible to know exactly the anatomy of the subject's heart.

4.1. USE OF X-RAYS

As already mentioned, during the ablation procedure the doctor must be guided in the various phases by an imaging technique that allows to correctly identify and treat the areas of interest without the risk of causing unwanted injury to the pulmonary veins or surrounding tissues. Conventional electrophysiology was initially based on fluoroscopy, an imaging technique that provides dynamic, real-time images of an anatomical region of interest and the location of the ablation and mapping catheters throughout the procedure (*Figure 22*) [32].

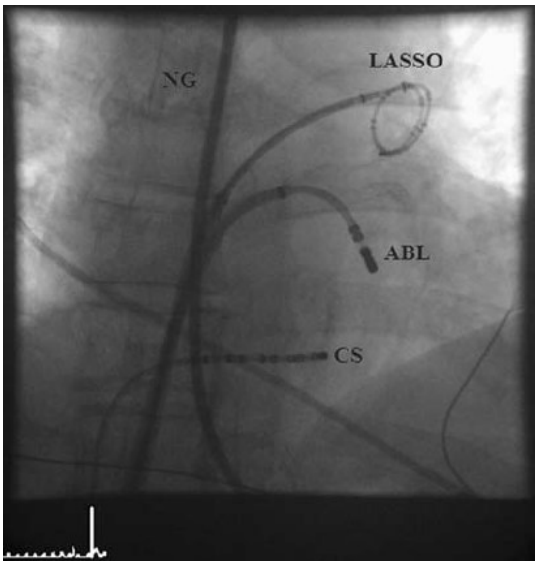

Figure 22: **Fluoroscopy visualization of ablation catheters in the left anterior oblique view.** ABL, ablation catheter; LASSO, circular mapping catheter; CS, coronary sinus catheter; NG, nasogastric tube [33].

Compared to normal X-ray systems, fluoroscopy allows to record the morphological changes of the heart in real time and to locate the catheters at the same time. Pulsed radiation is emitted, capturing sequential images at high frequencies. A fluorescent screen is used coupled to an image amplification system which converts it into a digital signal and sends it to a monitor in order to view the image.

The system, represented in *Figure 23*, consists of: an X-ray tube, an image intensifier, an image receptor, a computer for image processing and a monitor for viewing. The X-rays are projected to hit the patient lying on a special bed and the images are acquired by the receiver placed behind the patient. Collimators and anti-scatter grid are used to avid artifacts due to scattering effect resulting by hitting of X-rays on the patient. The support is C-shaped and has the ability to rotate in order to obtain projections from different angles. Once acquired the image, it is sent to an analog to digital converter and then processed by a digital computer. Finally the dinamic images will be visualized on a monitor by the doctor.

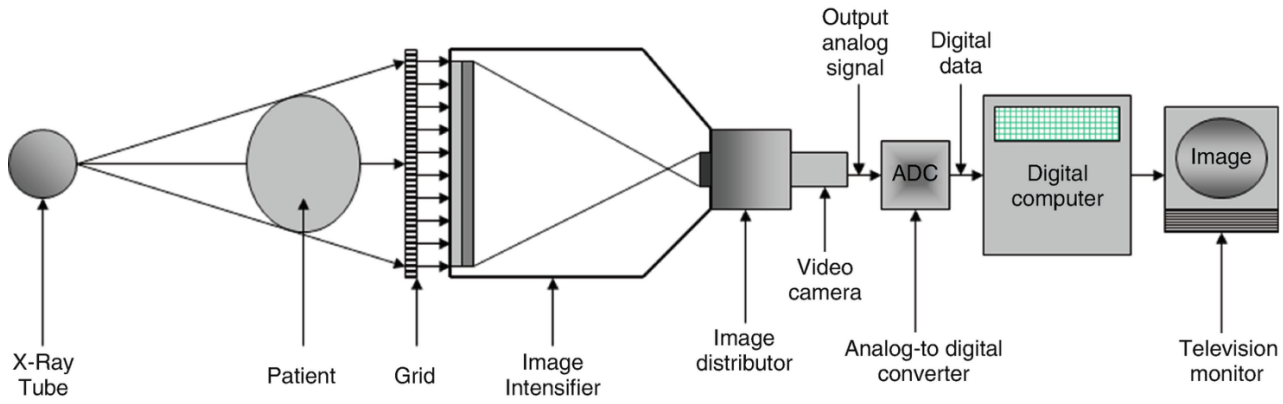

Figure 23: **Schematic of digital fluoroscopy system** [34]**.**

X-rays have the property of being absorbed more or less consistently in relation to the thickness and density of the obstacles they pass through. In particular, the bones of the body almost completely absorb the X-rays that strike them, creating a dark image on the screen. In fact, almost completely blocking the radiation on the screen there will be no fluorescence. The soft tissues, on the other hand, will project onto the screen images colored in gray, more or less dark, depending on the intensity. The images obtained will therefore have a color scale from black to white depending on the absorption characteristics of the organ they depict [34].

One of the limitations of the fluoroscopic system is the relatively difficulty of representing a three-dimensional structure of two dimensions, due to its relatively low resolution. However, if cardiac structures such as walls are poorly defined, foreign structures such as catheters are clearly visible.

Moreover, fluoroscopy involves the exposure, both of the patient and the doctor, to a non-negligible radiological risk. The effects due to overexposure to ionizing radiation have been studied and can be classified into stochastic and deterministic effects. Stochastic risks are called thresholdless since any dose, however small, is capable of producing biological damage. Furthermore, the likelihood of damage occurring or increasing is closely related to the increase in the administered dose. In particular, stochastic damage due to radiation can affect either the somatic cells or the cells of the germ tissues. In the first case the subject will undergo the development of neoplasms, while in the second there is the possibility that hereditary disorders and disorders will be generated. With regard to deterministic effects, on the other hand, we mean effects that occur in exposed individuals only if the dose was higher than a threshold value, typical for the effect considered, and the severity of which depends on the dose. They can be due to irradiation that has invested the whole body or can be localized only in some tissues. The proliferation of surviving cells is not sufficient to compensate for the damage caused by the radiation and therefore the inactivation of the cells results, which can cause a serious and clinically detectable loss of function in a tissue or organ.

In light of these risks, the American College of Cardiology said that a trade-off must always be struck between good resolution for imaging purposes and low radiation exposure. This compromise is precisely called ALARA (As Low As Reasonably Achievable), a principle based on which we try to administer the lowest possible radiation doses [35].

4.2. NON FLUOROSCOPIC MAPPING

Cardiac electrophysiology, despite being a relatively new science, has undergone a significant boost mainly thanks to new technologies to solve these problems.

An alternative to fluorescence is, for example, intracardiac echocardiography (ICE). It consists of a probe that is inserted intravenously and conducted to the right heart from which it is possible to acquire various projections that allow orientation and visualization of the patient's cardiac anatomy. ICE is based on the use of ultrasound emitted by a transducer (mechanical or electronic) positioned on the tip of the catheter (*Figure 24*).

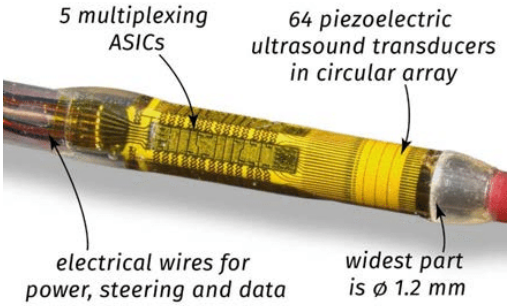

Figure 24: **Eagle Eye Platinum digital IVUS catheter developed by Philips.** It is the first intravascular imaging catheter. It is connected to the console through electrical wires that provides power and allow steering and data transmission. The tip is 1.2 mm wide and are present 64 piezoelectric transducers disposed on a circular array [36].

The principle that uses this type of technology is also known as the back reflection: the same probe works for both transmitting and receiving, unlike X-rays where you need to launch the pulse and have the receiver on the other side. The ultrasound system consists of different components (*Figure 25*): the probe, which is transmitting and receiving US to the tissues, and a processing unit, capable of processing the signals into diagnostic images. We also find a high voltage generator, i.e. the circuit in which the electronic signal is modeled to drive the transducer in generating US, which in turn are transmitted to the tissues. Once the impulse is sent, part of the energy will be reflected as echo waves and will bounce with different characteristics than those generated in relation to the structure of the obstacle it encountered. The same transducer then "hears" what is echoed by the target (such as a microphone, which transduces the mechanical wave into voltage), sending the detected signals to the Display processing unit, which will be able to reconstruct the image from it [36].

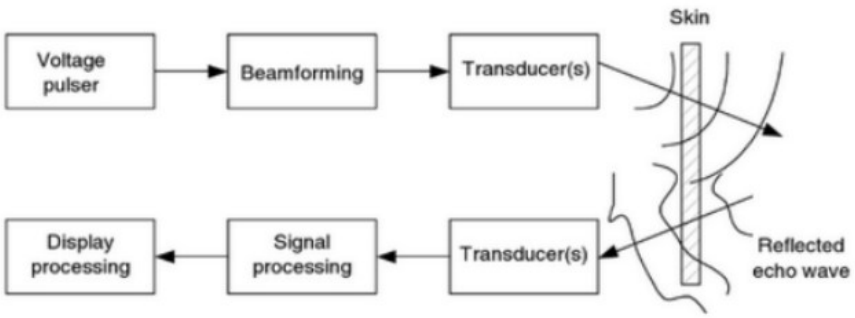

Figure 25: **Schematic of ultrasound system of ICE.**

The real revolution in the catheter ablation sector are the three-dimensional electroanatomical mapping systems (3D-EAM), which to date have become indispensable tools to guide ablative arrhythmia therapies as they are able to identify the temporal and spatial distribution of the myocardial electrical potential during a particular heart rhythm without excessive use of radiation.

Although originally applied only to relatively simple arrhythmias with a single target site (e.g. atrioventricular (AV) nodal reentry or tachycardias associated with Wolff-Parkinson-White syndrome), they have been increasingly used to address more complex arrhythmias in recent years, including atrial fibrillation, atrial flutter and ventricular tachycardia [37].

A mapping catheter is used, which as it moves within the heart will acquire the information necessary for ablation. These systems allow the recording of the localization of the lead, of the intracavitary ECG and other variables, in order to reconstruct in real time a 3D representation of the geometry of the heart chamber under study and to code with color maps the activation and the voltage in different areas of the myocardium.

The electroanatomical reconstruction of the heart chambers obtained using these new technologies is comparable to that obtained with the integration of pre-acquired radiological images with CT or MRI. This results in advantages for both the patient and the operator, who will no longer have to be exposed to radiation and a consequent reduction in the cost required for the procedure [29].

Several studies have confirmed how increasingly sophisticated systems guarantee a continuous and growing success of ablative procedures, the reduction of procedural times, the feasibility and safety of a zero or almost zero ray approach, and last but not least, a lower incidence of complications. peri and post procedural.

The three-dimensional electroanatomical mapping systems most representative of these technologies are EnSite (developed by St. Jude Medical, St Paul, MN, USA), Carto (Biosense Webster, Diamond Bar, CA, USA) and Rhytmia (Boston Scientific, Marlborough, MA, USA) [37].

4.2.1. ENSITE NAVIGATION SYSTEM, NAVX AND LAST VERSION VELOCITY

The system consists of:

- A set consisting of 3 pairs of adhesive skin patches
- A patch reference device
- 10 electrodes for surface ecg recording
- A computer module for data processing
- A display

The EnSite (*Figure 26*) combines the catheter localization system of a previous device (Medtronic's LocaLisa system) with the ability to create a 3D anatomical model of the heart chambers, using only information from a conventional electrophysiological study and skin patches [38].

Figure 26: **Ensite Precision™ Cardiac Mapping System** [39]**.**

This mapping mode is based on the passage of current through the chest (delivered through the skin patches) creating a voltage gradient (which also affects internal organs such as the heart) without creating any discomfort for the patient.

The voltage in a precise position within the vessels or heart can be recorded by the electrodes placed on a catheter and used by the system to determine the position of the catheter itself.

The 3 pairs of skin patches are applied on the body surface in order to recreate the 3 Cartesian axes of space (x, y, z). They are located opposite the thorax in anterior–posterior, left–right and cranio–caudal positions, as represented in *Figure 27*. Between them a low power current (350 mA) is alternately flowed, but with a frequency slightly different for each pair of electrodes.

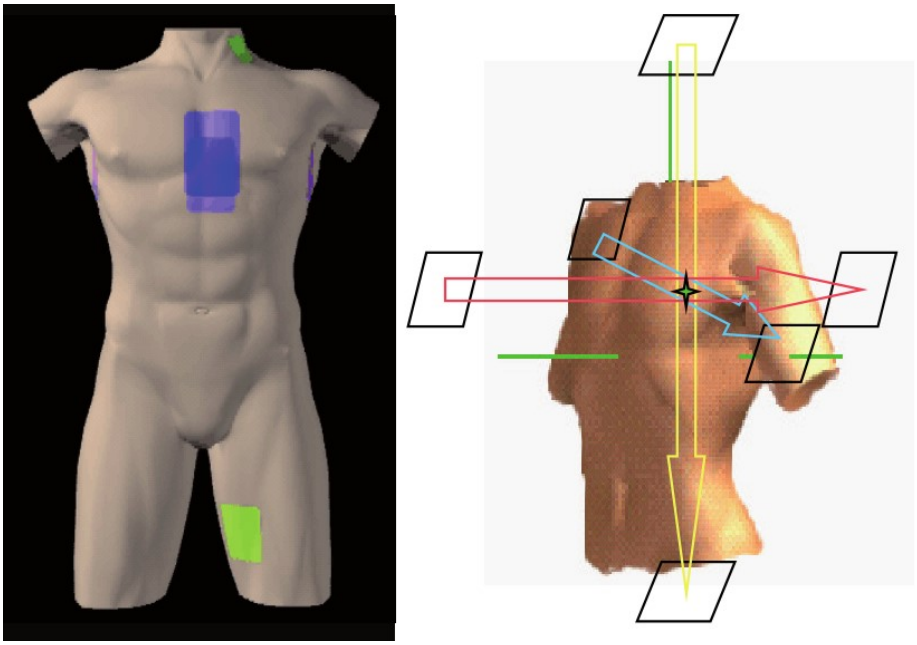

Figure 27: **Skin patches are applied on the body surface**. They are disposed in order to recreate the 3 Cartesian axes of space (x, y, z) [340].

The signals alternately picked up by the electrodes on the various catheters are digitally separated to measure the amplitude of each component at a different frequency and calculate the position according to each axis.

The characteristics of the 3 electric fields are calculated automatically by measuring the difference in signal amplitude between the pairs of skin patches and knowing the distance between them.

The position in the space of the electrodes on the catheters can therefore be differentiated by dividing each of the signal amplitudes (V) by the strength of the corresponding electric field (V/cm). Finally, the precise position of the tip of a catheter within the heart chamber is determined by considering the previous information and in relation to that of a reference electrode that is left fixed.

In this way, the EnSite system allows the real-time display of the position and movement of more than 12 catheters and 128 electrodes (Velocity) simultaneously present in the heart [37].

Localization and Positioning

EnSite allows the rapid creation of detailed anatomical models. Sequential placement of a catheter at different sites along the endocardial surface of a heart chamber allows to establish the geometry of that chamber. The system is in fact able to acquire points relating to the position of a catheter 96 times per second.

The geometry of the chamber is reproduced after sampling a few thousand points. The virtual anatomical geometry is acquired by moving the catheter in all directions within the heart chamber under examination, maintaining contact with the endocardial surface.

An algorithm then defines the reconstruction using the most distant points for each corner from the geometric center, which can be chosen by the operator or defined by the system. In addition, the operator can specify some fixed points during the acquisition of the geometry to highlight the areas where the catheter has come into contact with the endocardium (these points cannot be eliminated and guide the algorithm in defining the surface) .

Finally, the map is improved by an interpolation that smooths the rendering of the 3D reconstruction of the studied heart chamber.

Electrophysiology

The control of the variability related to the cardiac cycle is entrusted to the fact that the acquisitions are synchronized with the surface ECG.

In addition to this control, the Velocity system also includes a compensation of movements due to respiratory acts, which is based on the identification of breath-dependent changes in thoracic impedance.

The system is able to analyze the activation and the voltage, timed over 10 beats, for each acquired point and then display the variations in activation or voltage on the 3D map of the heart chamber with a color code. It is also possible to save the map thus obtained for subsequent checks.

This technique represents the preferred approach to study inducible, sustained and hemodynamically well tolerated tachyarrhythmias by the patient. In patients with non-inducible or

non-haemodynamically tolerable arrhythmias, the voltage map obtained by analyzing the voltage at points of interest is sufficient to plan the ablation strategy [41].

EnSite and cardiac CT/MRI

The EnSite platform supports the fusion of electrophysiological sampling data with previously acquired imaging, such as cardiac CT or MRI (EnSite Digital Image Fusion), in order to obtain more detailed maps of the specific patient anatomy, adding anatomical references to guide more precisely the procedure.

The EnSite Velocity allows, in addition to previous versions, to collect and display data from two different heart chambers simultaneously. Another important feature of the Velocity version is the integration with Hansen technology, which allows you to view the contact force of the catheter tip with the heart walls on the display during the procedure.

The procedures guided by the EnSite system can be performed with the same catheters that can also be used in the conventional fluoroscopic approach. EnSite is in fact an open system, in which different types of catheter, built by different companies, including those for cryoablation, can be used.

The system is able to locate the position of the catheters from the moment they are inserted into a blood vessel, so the use of fluoroscopy can be eliminated or reduced even for the first stages of positioning. Additionally, a point of interest or ablation site tag can be added at any time during the procedure to help visualize conduction block lines accurately.

The radiofrequencies delivered during ablation do not interfere with the mapping or localization system of the catheters.

4.2.2. CARTO ELECTROANATOMICAL MAPPING SYSTEM AND LAST VERSION CARTO 3

The Carto system consists of:

- A low intensity magnetic field generator (consisting of 3 coils that are positioned below the patient's chest)
- A reference skin patch fixed on the patient's back
- A computer to process the data
- A display

The Carto system requires specific catheters in order to generate 3D electroanatomical maps of the heart chambers. These catheters are characterized by the presence, near the tip, of specific localization sensors, composed of spirals positioned orthogonally to each other according to the 3 axes of space (*Figure 28*).

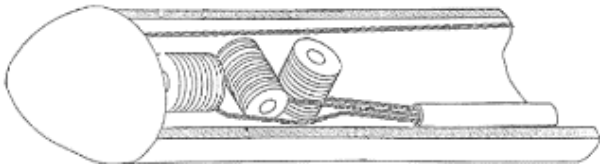

Figure 28: **Catheter localization sensor.** It is composed of three spirals positioned orthogonally to recreate the 3 Cartesian axes of space (x, y, z) [42].

This system uses magnetic fields to determine catheter position and orientation, and records intracavitary ECGs from the electrodes at the catheter tip. The sampling of spatial and electrical information from different points allows the 3D reconstruction of the heart chamber, the real-time analysis of the arrhythmia mechanism and the substrate to be ablated.

Electroanatomical mapping is based on the premise that a metal spiral generates an electric current when placed in a magnetic field, as shown in *Figure 29*. The intensity of this current depends on the strength of the magnetic field and on the orientation of the spiral that acts as a sensor [38].

Figure 29: **Magnetic field generator** [42]**.**

The Carto system uses a triangulation algorithm similar to that used by the GPS (Global Positioning System). The sensors in the tip of the catheter detect the intensity of the current developed in each spiral (x, y, z) and the system identifies the distance of the catheter from each of the generators of the magnetic field. The possible position of the catheter with respect to each source develops as a spherical cap with a radius equal to the distance detected by the sensor; however, the catheter can only be located in the space shared by the intersection of the spheres built from the 3 magnetic field generators (*Figure 30*).

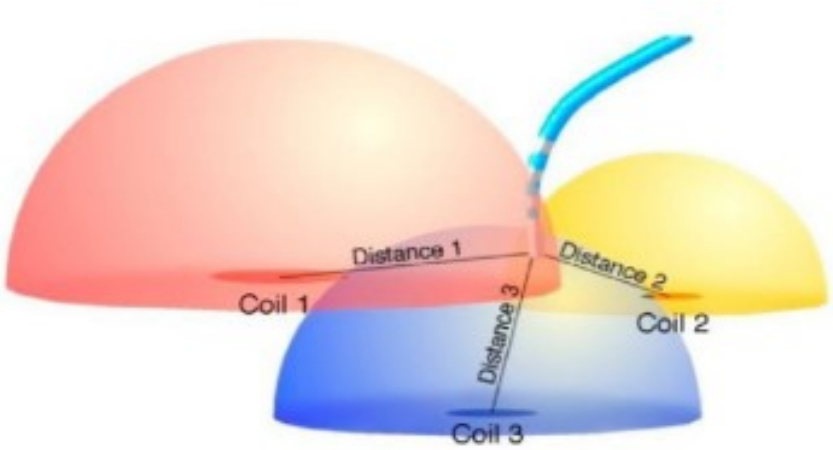

Figure 30: **Catheter localization principle in Biosense CARTO electroanatomic mapping system.** Three separate coils emit a low-level magnetic field, diagrammatically represented by color-coded hemispheres. The field strength from each coil is measured by a sensor within the tip of a specialized mapping/ablation catheter, and its position relative to each coil is then triangulated [37].

In addition to the x, y, z coordinates, the Carto system can also determine the roll, yaw and pitch of the catheter.

Intracavitary electrocardiograms are recorded by the catheter and integrated with position information for each endocardial site reached. Using this approach, the local tissue activation recorded by touching different sites progressively allows the creation of the activation and geometric map of the heart chamber.

The Carto system compensates for artifacts due to the movements of the heart cycle and breathing through several adjustment steps: it corrects the coordinates of the map using the surface electrocardiogram and anatomical tags as a reference.

The surface ECG is used to synchronize the activation data recorded by the tip of the catheter during the creation of the map. The anatomical reference is a catheter that is left fixed in a specific position within the heart or more often it is a skin patch applied to the patient's back; the movements of the anatomical reference reflect the movement of the patient's rib cage and can be used to correct distortions during the creation of the electroanatomical map [43].

Finally, there is a need for a third variable to be set to ensure the reliability of the system, the so-called window of interest. It is defined as the time interval, in relation to a reference point on the surface ECG, in which local activation occurs, which can be considered early or late compared to the reference. The total length of the window of interest cannot exceed the cycle of tachycardia studied.

The Carto system offers the possibility of merging the electroanatomical map obtained with CT or MRI images acquired before the procedure, this allows to verify anatomical references, improve cardiac geometry and guide ablation more precisely [43].

In the latest version, Carto 3, it is also possible to use 2 other modules. The Carto UNIVU module that allows you to merge fluoroscopic images with the electroanatomical map generated in real time, and the Carto Sound module that allows you to use intracardiac ultrasound both as a method of monitoring the procedure and as an anatomical aid in construction [44].

4.2.3. RHYTHMIA NAVIGATION SYSTEM

The Rhythmia mapping system (*Figure 31.a*) consists of:

- Mapping catheter
- Workstation
- Signal processing module
- Magnetic field generator
- Dorsal patch for selection reference

A high-resolution catheter is used, the IntellaMap Orion. This has the structure of a basket catheter with 64 electrodes which allows rapid high-density mapping of the heart cavities, as represented in *Figure 31.b* [46].

Spatial localization and geometric reconstruction take place also in this case thanks to the generation of a magnetic field. The generator is placed under the table on which the patient is standing.

Figure 31: **Rhythmia mapping system. (a)** RHYTHMIA HDx™ Mapping System. **(b)** INTELLAMAP ORION™ High-Resolution Mapping Catheter [45].

The reference patches are attached with an adhesive on the subject's back, in correspondence with the cardiac shadow. These perform the important function of highlighting the patient's movements with respect to the magnetic field and of supporting the electric field for viewing conventional scaling and diagnostic catheters without magnetic sensors.

During the procedure, the signal processing module takes intracardiac signals from the diagnostic catheters and/or scalers, and from the surface electrodes, as input and sends them to the workstation. Finally, here the data acquired by the catheters are processed in order to create the images and obtain a cardiac map [38].

5. A NEW INDEX FOR ECTOPIC FOCUS IDENTIFICATION

5.1. DATA

The data used in this thesis were taken from the EDGAR Database and refer to a 2016 study in which the accuracy of the non-invasive estimation of the dominant frequencies and the determination of electrical patterns through the inverse problem were evaluated.

The data set consists of the signals and geometric networks of two patients suffering from atrial fibrillation acquired in order to implement a resolution of the arrhythmia through catheter ablation. Multi-channel electrocardiograms (ECGs) were recorded for mapping of body surface potential (BSPM) with a custom vest of 54 thoracic ECG leads, as depicted in *Figure 32*.

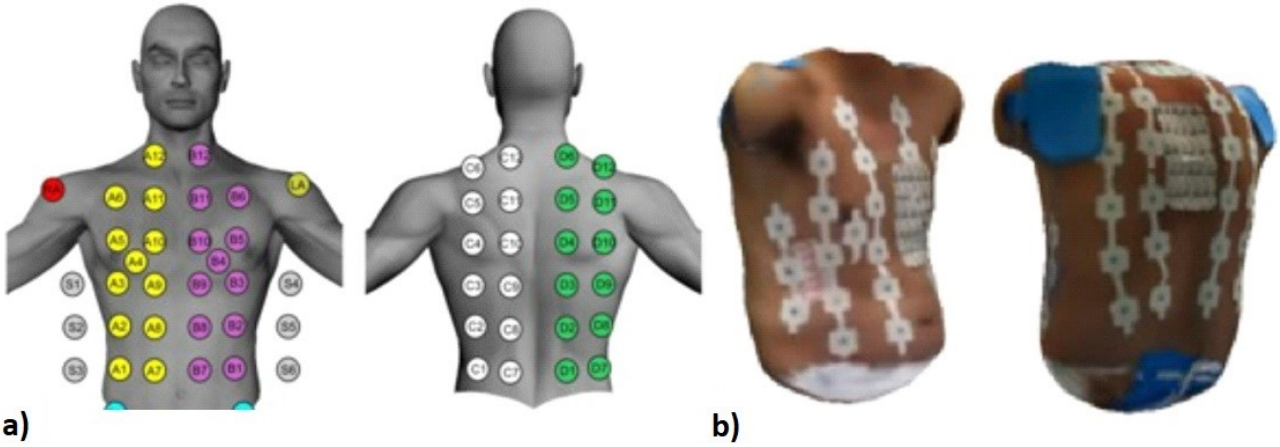

Figure 32: **Custom-made vest with 54 thoracic ECG leads. (a)** ECG signals were electrically referenced at Wilson Central Terminal (WCT), recorded with two electrodes on the shoulders and one electrode in the lower left torso. **(b)** 3D model of the custom-made vest [47].

Body Surface Potential Mapping signals were recorded simultaneously with endocardial recordings with high resolution multipolar catheters. In particular, a 64-pole basket catheter (Constellation, Boston Scientific, Natick, MA, USA) located sequentially on the right and left atria. Additionally, a standard tetrapolar catheter was placed in the coronary sinus and a 20-pole catheter in the opposite atrium to the basket catheter. The electroanatomical mapping system used is the CARTO system (CARTO XP, version 7.7; Biosense-Webster), with incorporated spectral capabilities that allowed the analysis of dominant frequencies in real time.

In order to avoid ventricular electrical activity, BSPM signals were recorded during an Adenosine bolus infusion that blocked the atrioventricular node providing 6-7 s of atrial signals without ventricular activity [47].

5.2. DATA PROCESSING

For the data analysis, the software for numerical calculation and statistical analysis MATLAB was used. The meshes of the Torso and Atria of the two patients were loaded and represented. The points on the surface of the atria where the mapping catheter stopped for the acquisition of information were highlighted, distinguishing them in relation to the value of the recorded potential.

For the potential data, both ECGs and EGMs were sampled at a rate of 2034.5 Hz. Each signal was associated with its relative acquisition point, both on the surface of the body and on the epicardium of the heart chamber and analyzed in frequency. The signals were filtered with a third order Butterworth filter with cut-off frequency equal to 0.5 Hz and 30 Hz.

For each signal, both Dominant Frequency (DF, Hz) and Spectral Area (SA, V·Hz) were computed. The DF was obtained by calculating the maximum frequency in the band between 4-10 Hz, for each recording acquired. The SA, on the other hand, was obtained by calculating the area of the spectrum in the frequency band between 4 Hz and 10 Hz for each recording acquired.

5.3. STATISTICS

From the literature it emerged that the DF, usually present in the frequency band between 4-10 Hz, is a valid indicator for identifying the ectopic focuses of atrial fibrillation, in this study we tried to find an alternative indicator with respect to frequencies, such as the area of the spectrum, that is less prone to disturbances. Specifically, in these two subjects, the DF was higher than 7 Hz near the ectopic focuses, as represented in *Figure 33*.

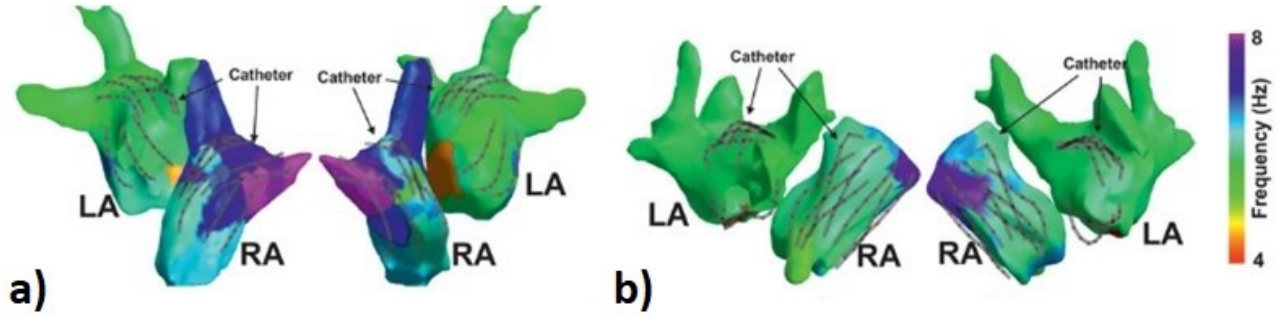

Figure 33: **Dominant Frequency (DF) map. (a)** Atria dominant frequency map of the first patient; **(b)** Atria dominant frequency map of the second patient**.** [47]

Having assumed the DF as the gold standard, the acquisitions points on the surface were classified as near and far from the ectopic focuses according with their values of DF. Specifically, points with DF higher than 7Hz were classified as near while points with DF lower that 7 Hz were classified as far.

In order to evaluate their clinical utility, the DF and SA values of the two classes were compared. The first, the *Wilcoxon Rank-Sum Test*, was performed in order to evaluate statistical difference ($p<0.05$) between the two classes. Secondly, the *Receiver Operating Characteristic (ROC)* was used to evaluate the SA ability to discriminate the points and to find the optimal threshold (OT, V·Hz). OTs were defined at the point where sensitivity and specificity are equal.

Finally, the *Two One-Sided Test (TOST)*, was performed in order to evaluate if DF and SA values computed from EGMs can be considered similar to those computed from ECGs.

5.4. RESULTS

5.4.1. ATRIA

5.4.1.1. FIRST PATIENT

In *Figure 34* is shown the tridimensional structure of the Atria, with and without the acquisition point highlighted, of the first patient.

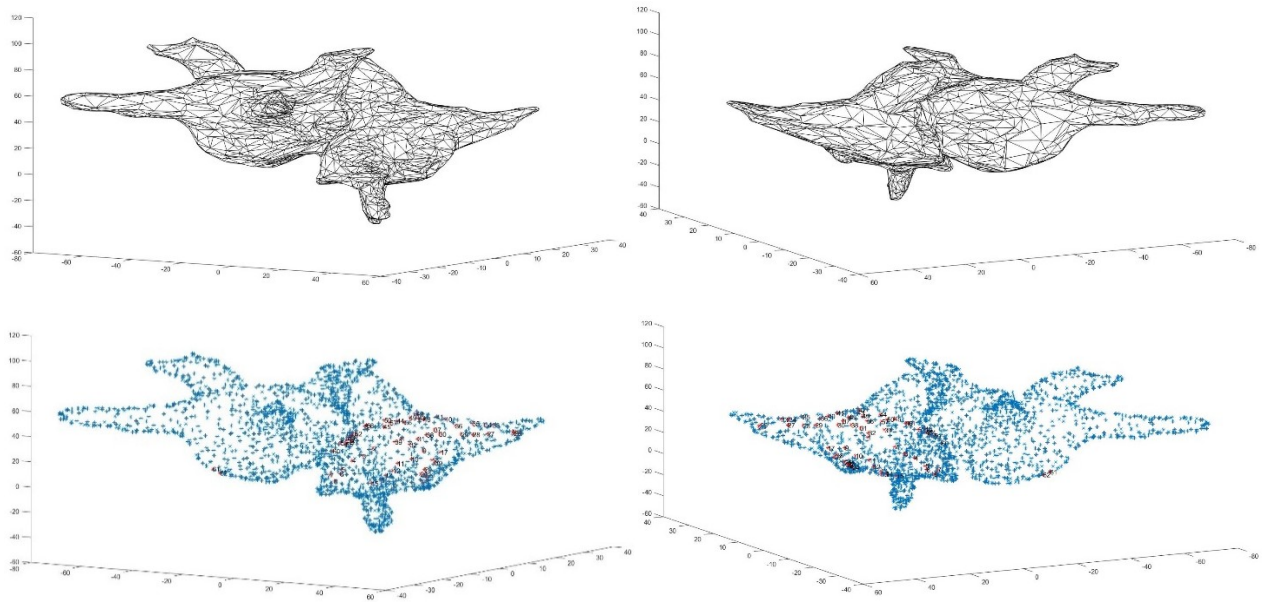

Figure 34: **Tridimensional geometries of the Atria.** Upper images represent Atria tridimensional geometry of first patient (anterior and posterior view); Lower images represent Atria tridimensional geometry of first patient (anterior and posterior view).

Table 2 shows the results of the DF and SA relative to the acquisition points of the EGM recordings in the 4-10 Hz frequency band of the first patient.

EGM	**TOT**	**NEAR**	**FAR**	
	MEDIAN [25th 75th]	**MEDIAN [25th 75th]**	**MEDIAN [25th 75th]**	**P-value**
DF [Hz]	6.43 [6.29 7.37]	7.50 [7.30 8.04]	6.43 [6.29 6.43]	-
SA [%]	11.47 [8.33 19.50]	19.70 [17.25 27.39]	8.88 [7.67 11.76]	3.0695e-08

Table 2: **Results related to the EGMs recordings of the first patient.** The table shows the median value **(MEDIAN)** and the **25th** and **75th** percentiles, respectively, of all the points acquired **(TOT)**, **NEAR** if the potential recorded is >7 Hz and **FAR** if <7 Hz. The values of the f waves dominant frequencies **(DF)** are expressed in Hz, instead the values of the and Spectral Area **(SA)** are expressed in %. In the last column is reported the **P-value.**

As regards the ROC analysis, a value of the *area under the curve* equal to 0.92 was obtained with an *OT* of 14.78 V·Hz, represented in *Figure 35.*

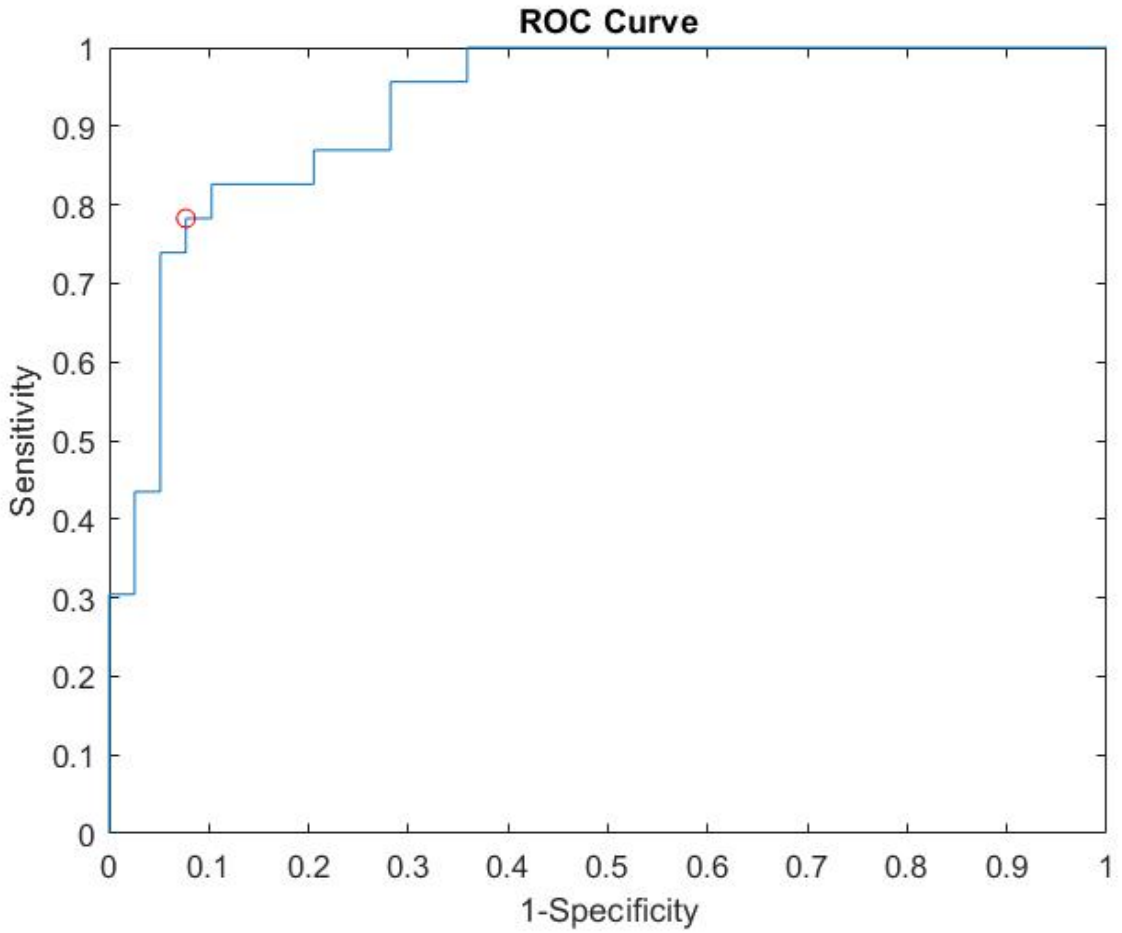

Figure 35: **ROC Curve.** The red dot indicates the optimal cut-off point relative to the f wave dominant frequency and percentage of spectrum distributions.

Figure 36 and *Figure 37* shows a comparison between the points on the surface of the atria, where the mapping catheter stopped during the acquisition, obtained in relation to the value of the potential recorded and the value of the and Spectral Area.

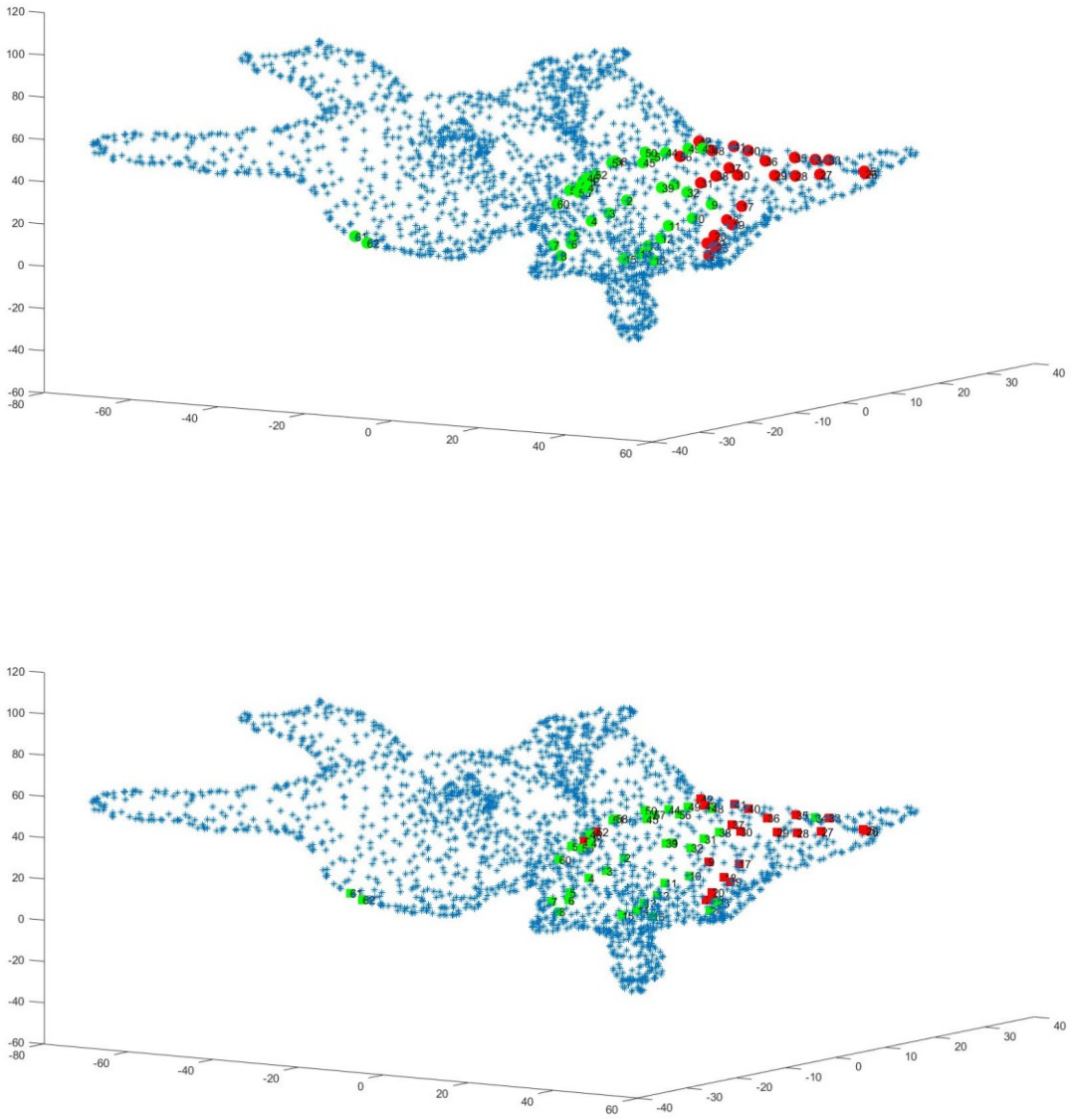

Figure 36: **Atria dominant frequency map of the first patient.** The points highlighted on the surface indicate where the mapping catheter stopped for the acquisition of information and are represented with different colors in relation to the potential value recorded: *Red* if the potential recorded is >7 Hz and *green* if <7 Hz. In the upper image there is the Atria SA map of first patient (anterior view); in the lower image there is the Atria DF map of first patient (anterior view).

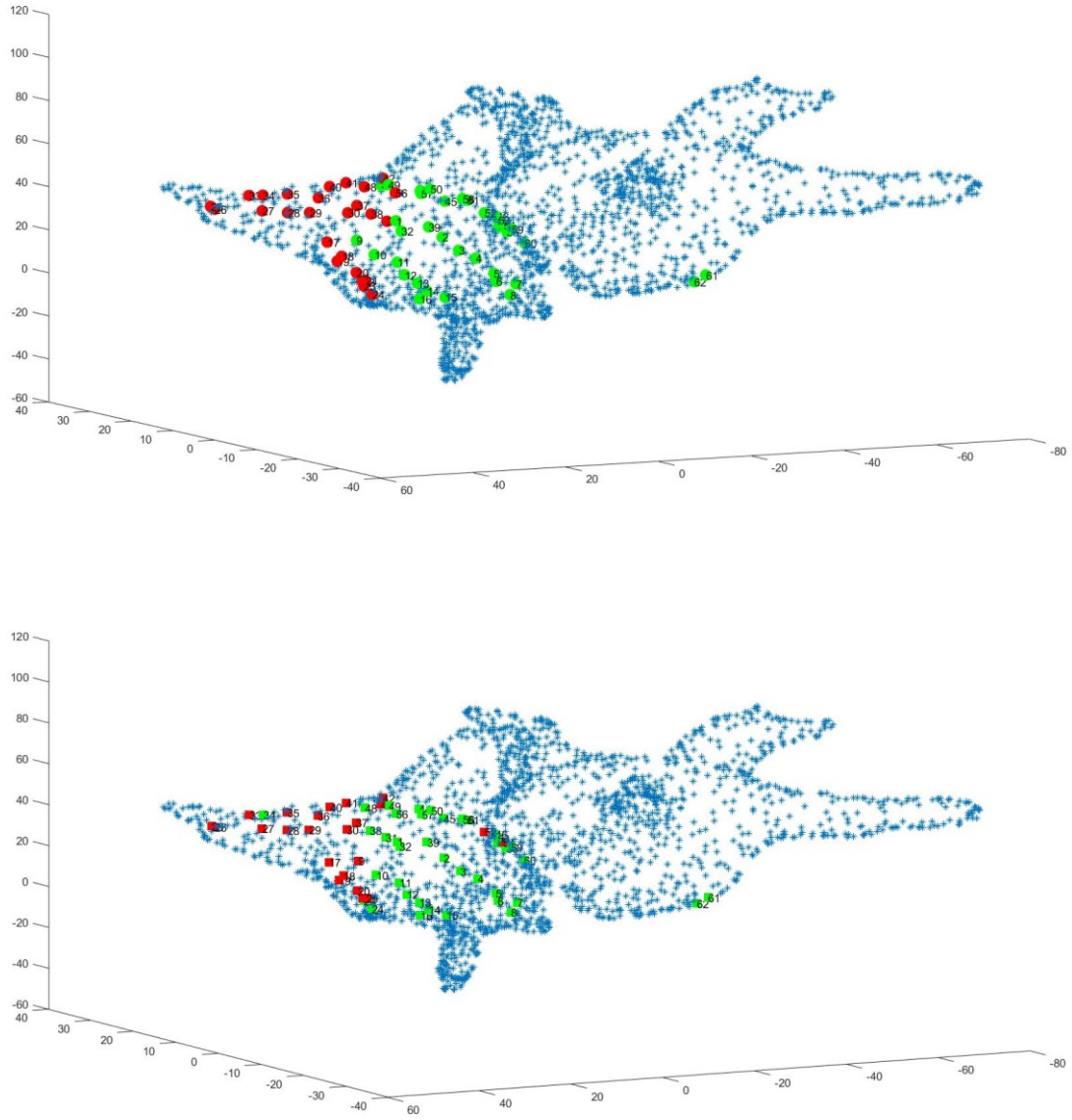

Figure 37: **Atria dominant frequency map of the first patient.** The points highlighted on the surface indicate where the mapping catheter stopped for the acquisition of information and are represented with different colors in relation to the potential value recorded: *Red* if the potential recorded is >7 Hz and *green* if <7 Hz. In the upper image there is the Atria SA map of first patient (posterior view); in the lower image there is the Atria DF map of first patient (posterior view).

5.4.1.2. SECOND PATIENT

In *Figure 38* is shown the tridimensional structure of the Atria, with and without the acquisition point highlighted, of the second patient.

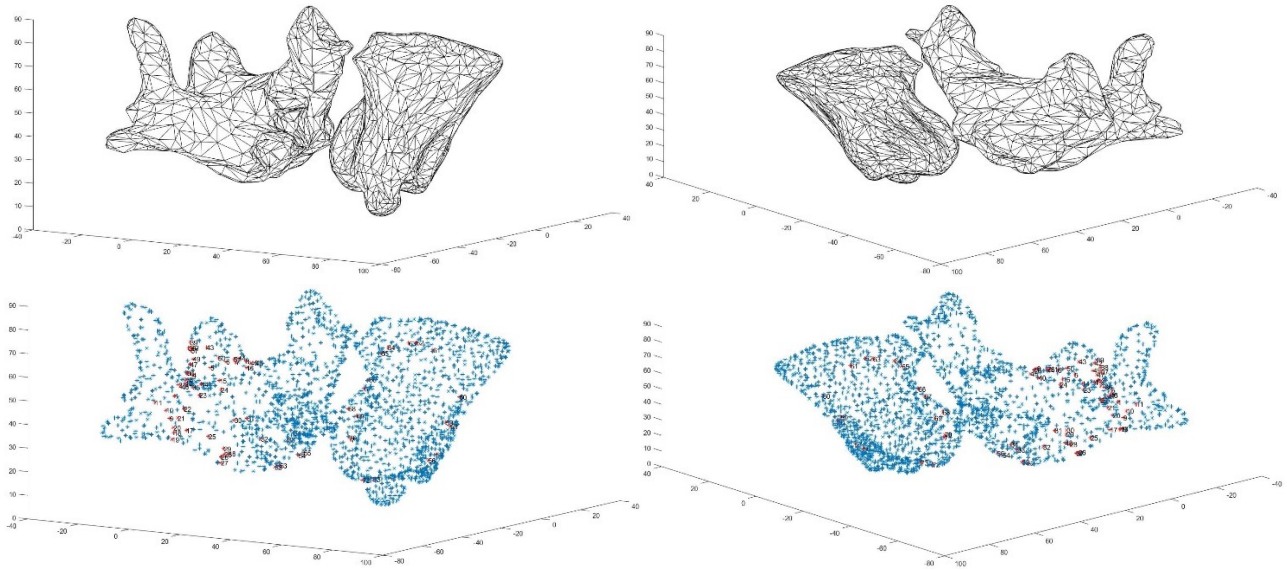

Figure 38: **Tridimensional geometries of the Atria.** Upper images represent Atria tridimensional geometry of second patient (anterior and posterior view); Lower images represent Atria tridimensional geometry of second patient (anterior and posterior view).

Table 3 shows the results of the DF and SA relative to the acquisition points of the EGM recordings in the 4-10 Hz frequency band of the second patient.

EGM	**TOT**	**NEAR**	**FAR**	
	MEDIAN [25th 75th]	**MEDIAN [25th 75th]**	**MEDIAN [25th 75th]**	**P-value**
DF [Hz]	5.40 [4.91 6.38]	8.35 [7.20 9.49]	5.40 [4.91 5.52]	-
SA [%]	20.07 [16.95 24.28]	25.16 [21.53 26.51]	19.24 [16.81 23.62]	0.0145

Table 3: **Results related to the EGMs recordings of the second patient.** The table shows the median value **(MEDIAN)** and the **25th** and **75th** percentiles, respectively, of all the points acquired **(TOT)**, **NEAR** if the potential recorded is >7 Hz and **FAR** if <7 Hz. The values of the f waves dominant frequencies **(DF)** are expressed in Hz, instead the values of the and Spectral Area **(SA)** are expressed in %. In the last column is reported the **P-value.**

As regards the ROC analysis, a value of the *area under the curve* equal to 0.76 was obtained with an *OT* equal to 22.99 V·Hz, represented in *Figure 39*.

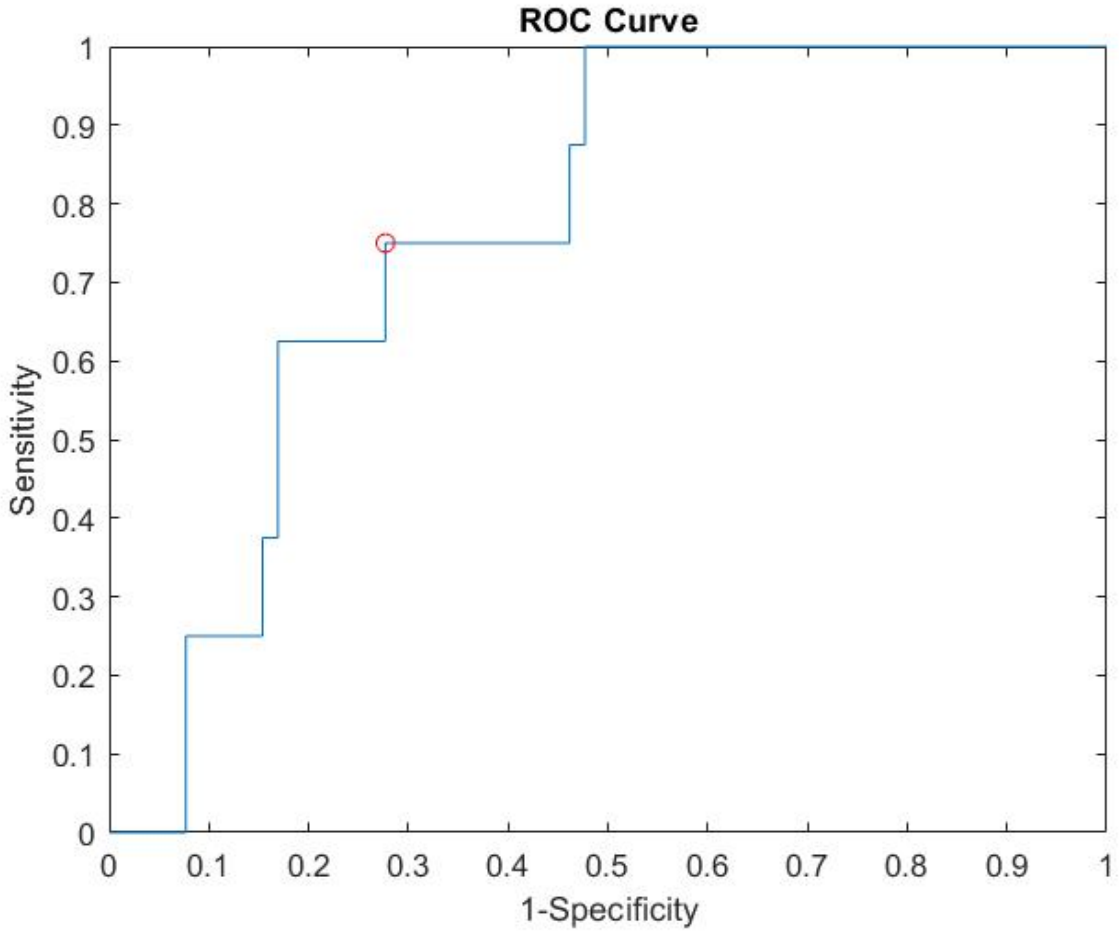

Figure 39: **ROC Curve.** The red dot indicates the optimal cut-off point relative to the f wave dominant frequency and percentage of spectrum distributions.

Figure 40 and *Figure 41* show a comparison between the points on the surface of the atria, where the mapping catheter stopped during the acquisition, obtained in relation to the value of the potential recorded and the value of the and Spectral Area.

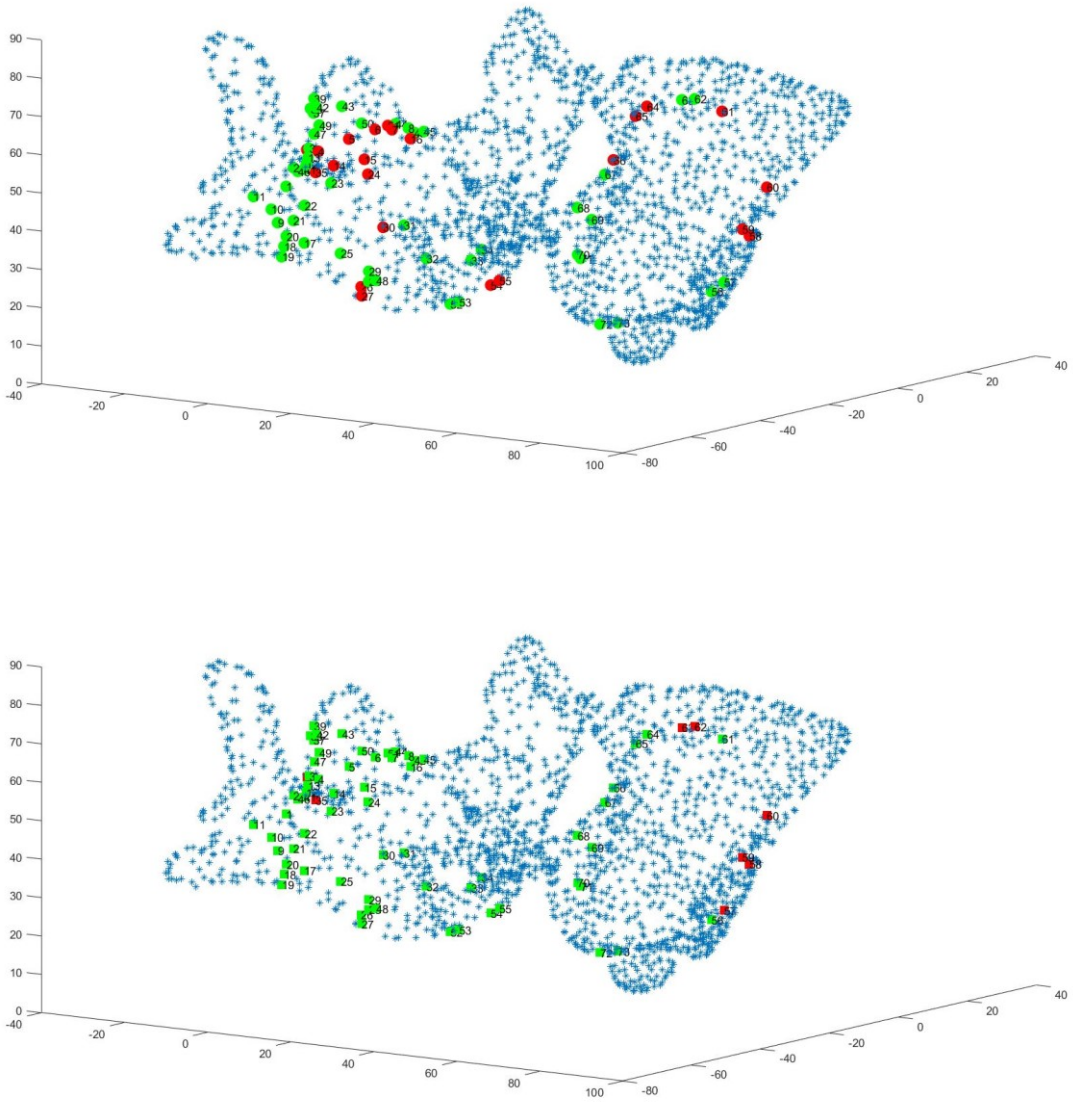

Figure 40: **Atria dominant frequency map of the second patient.** The points highlighted on the surface indicate where the mapping catheter stopped for the acquisition of information and are represented with different colors in relation to the potential value recorded: *Red* if the potential recorded is >7 Hz and *green* if <7 Hz. In the upper image there is the Atria SA map of second patient (anterior view); in the lower image there is the Atria DF map of second patient (anterior view).

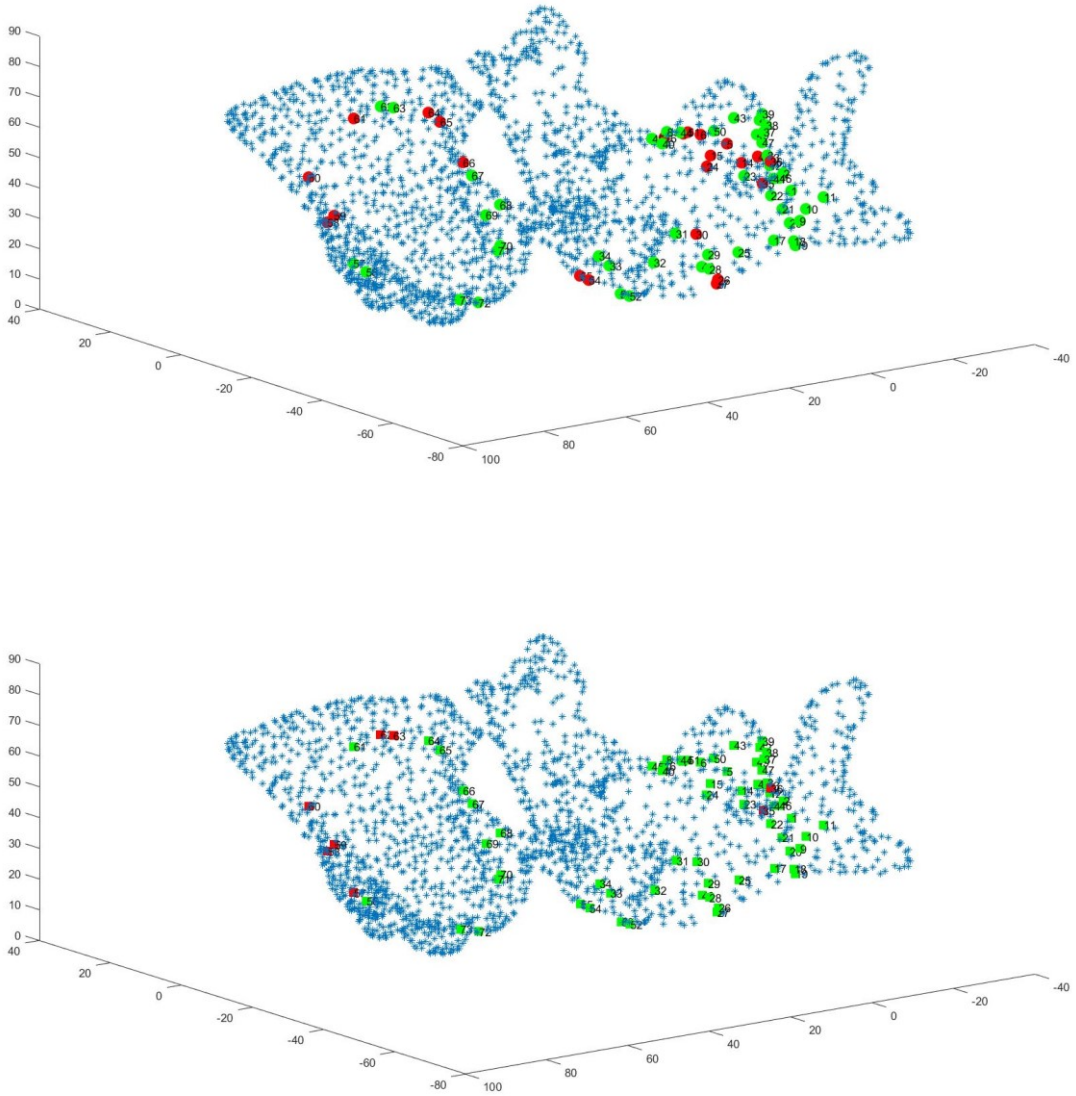

Figure 41: **Atria dominant frequency map of the first patient.** The points highlighted on the surface indicate where the mapping catheter stopped for the acquisition of information and are represented with different colors in relation to the potential value recorded: *Red* if the potential recorded is >7 Hz and *green* if <7 Hz. In the upper image there is the Atria SA map of second patient (posterior view); in the lower image there is the Atria DF map of second patient (posterior view).

5.4.2 TORSO

5.4.2.1. FIRST PATIENT

In *Figure 42* is shown the tridimensional structure of the Atria, with and without the acquisition point highlighted, of the first patient.

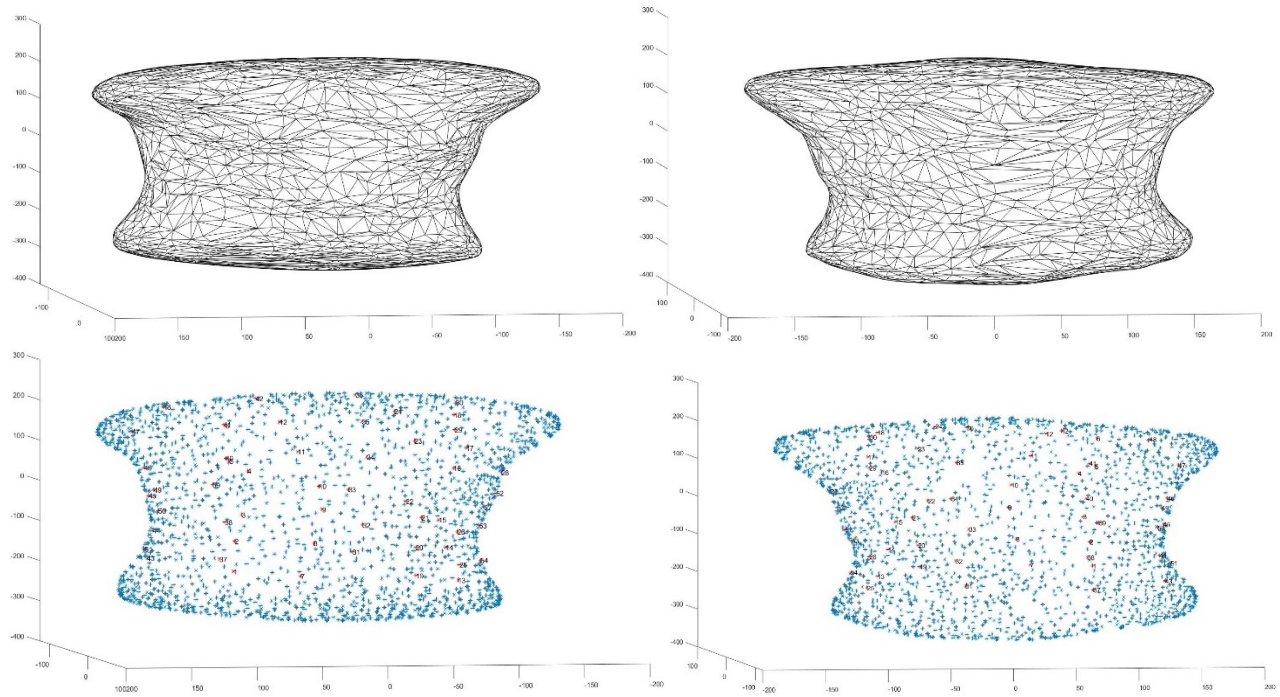

Figure 42: **Tridimensional geometries of the Torso.** Upper images represent Torso tridimensional geometry of first patient (anterior and posterior view); Lower images represent Torso tridimensional geometry of first patient (anterior and posterior view).

Table 4 shows the results of the DF and SA relative to the acquisition points of the ECG recordings in the 4-10 Hz frequency band of the first patient.

ECG	**TOT**	**NEAR**	**FAR**	
	MEDIAN [25th 75th]	**MEDIAN [25th 75th]**	**MEDIAN [25th 75th]**	**P-value**
DF [Hz]	6.83 [6.56 6.83]	7.17 [7.10 7.53]	6.83 [6.56 6.83]	-
SA [%]	3828.10 [3253.60 4543.20]	4366.60 [2952.30 5688.70]	3828.10 [3254.90 4445.60]	0.6497

Table 4: **Results related to the ECG recordings of the first patient.** The table shows the median value **(MEDIAN)** and the **25th** and **75th** percentiles, respectively, of all the points acquired **(TOT)**, **NEAR** if the potential recorded is >7 Hz and **FAR** if <7 Hz. The values of the f waves dominant frequencies **(DF)** are expressed in Hz, instead the values of the and Spectral Area **(SA)** are expressed in %. In the last column is reported the **P-value.**

As regards the ROC analysis, a value of the *area under the curve* equal to 0.55 was obtained with an *OT* equal to 3845.30 V·Hz, represented in *Figure 43.*

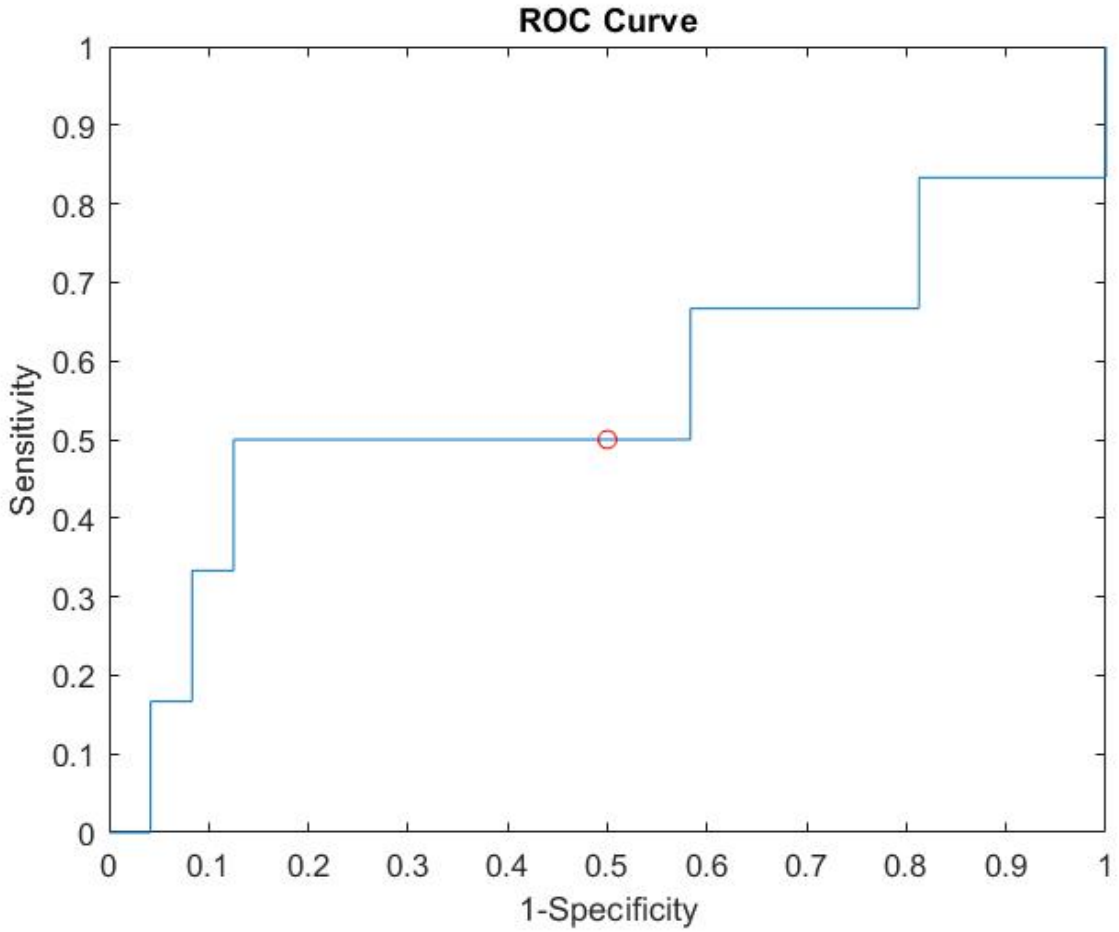

Figure 43: **ROC Curve.** The red dot indicates the optimal cut-off point relative to the f wave dominant frequency and percentage of spectrum distributions.

Figure 44 and Figure 45 show a comparison between the points on the surface of the torso, where the mapping catheter stopped during the acquisition, obtained in relation to the value of the potential recorded and the value of the and Spectral Area.

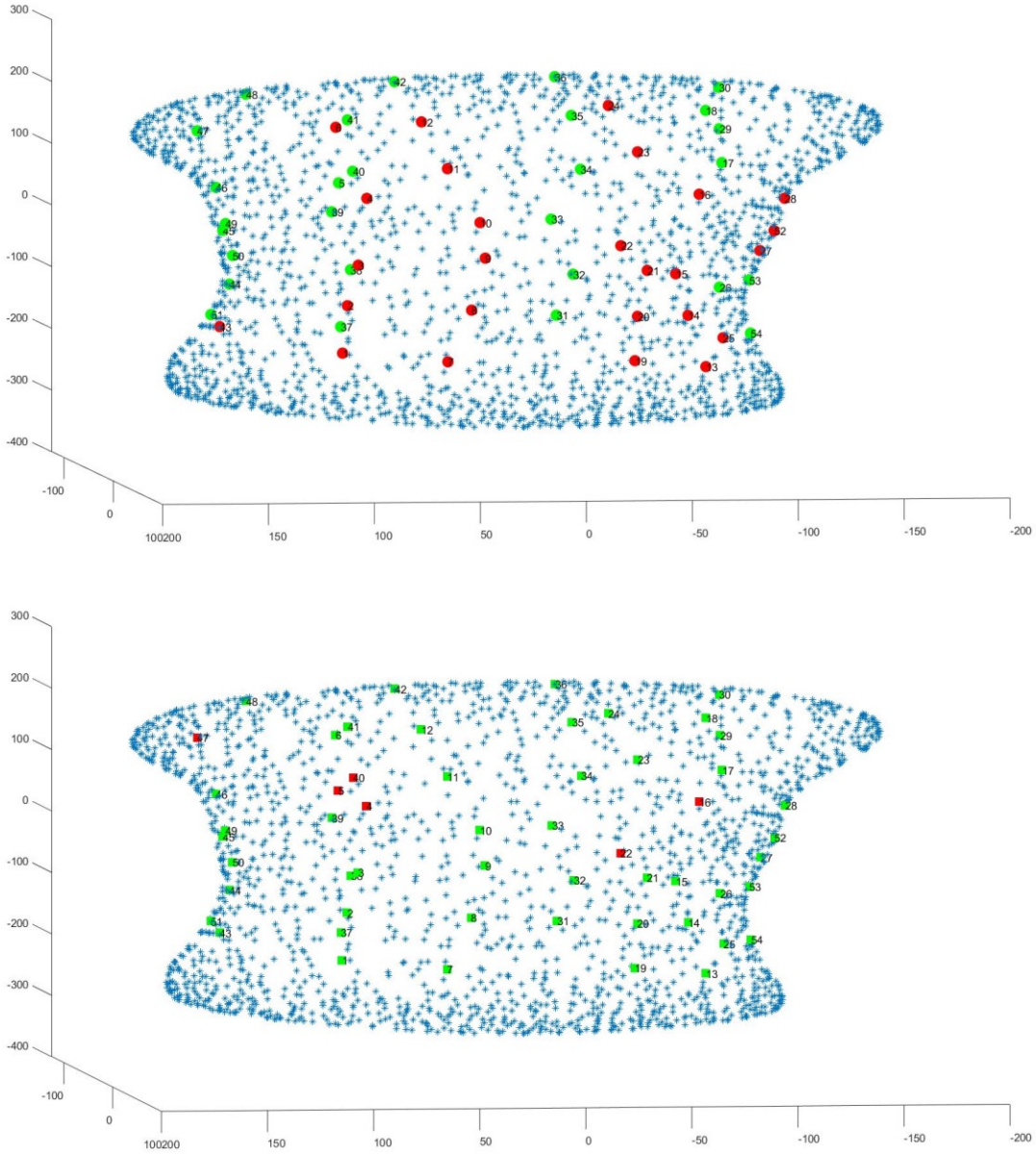

Figure 44: **Torso dominant frequency map of the first patient.** The points highlighted on the surface indicate where the mapping catheter stopped for the acquisition of information and are represented with different colors in relation to the potential value recorded: *Red* if the potential recorded is >7 Hz and *green* if <7 Hz. In the upper image there is the Torso SA map of first patient (anterior view); in the lower image there is the Torso DF map of first patient (anterior view).

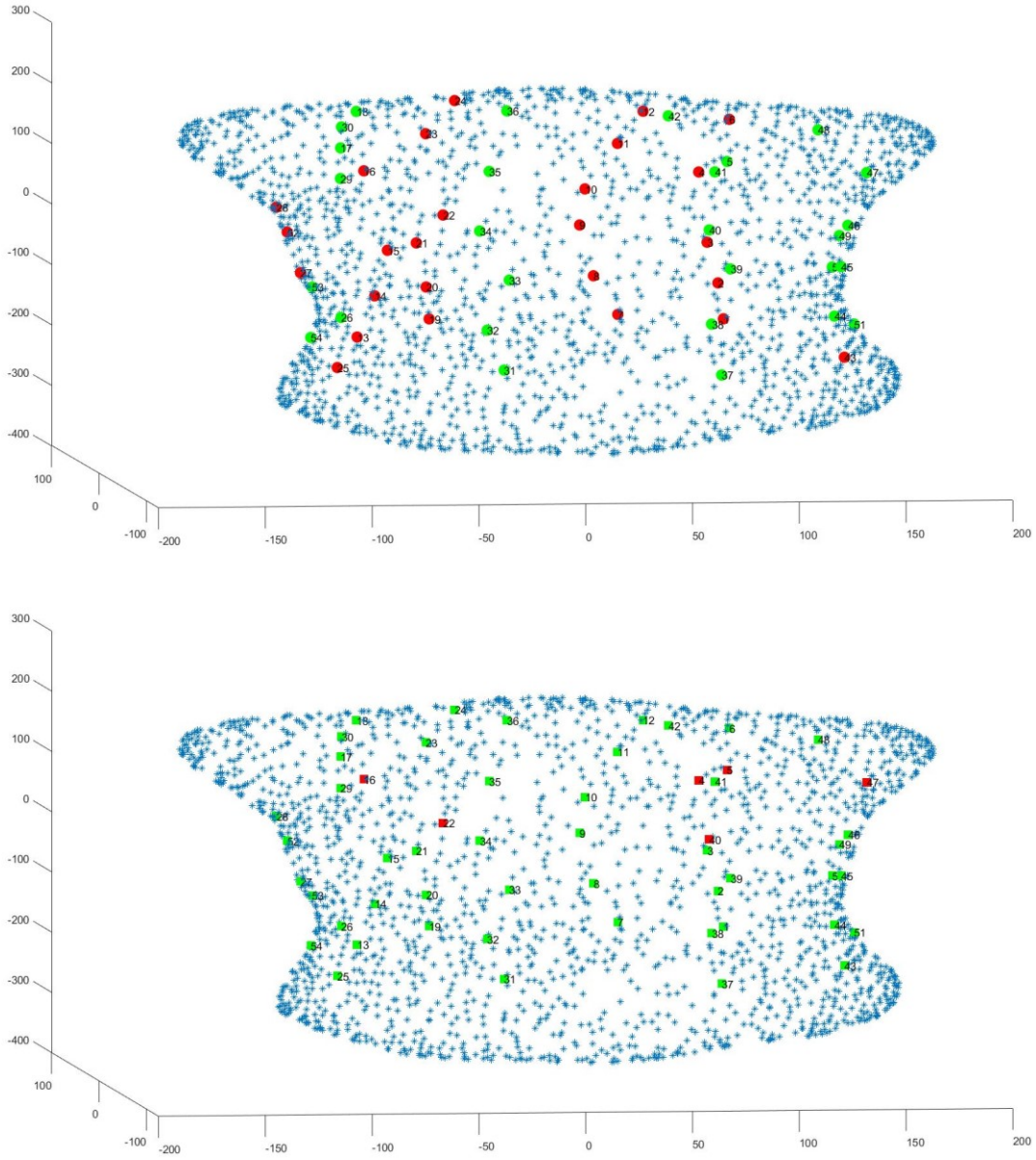

Figure 45: **Torso dominant frequency map of the first patient.** The points highlighted on the surface indicate where the mapping catheter stopped for the acquisition of information and are represented with different colors in relation to the potential value recorded: *Red* if the potential recorded is >7 Hz and *green* if <7 Hz. In the upper image there is the Torso SA map of first patient (posterior view); in the lower image there is the Torso DF map of first patient (posterior view).

5.4.2.2. SECOND PATIENT

In *Figure 46* is shown the tridimensional structure of the Torso, with and without the acquisition point highlighted, of the second patient.

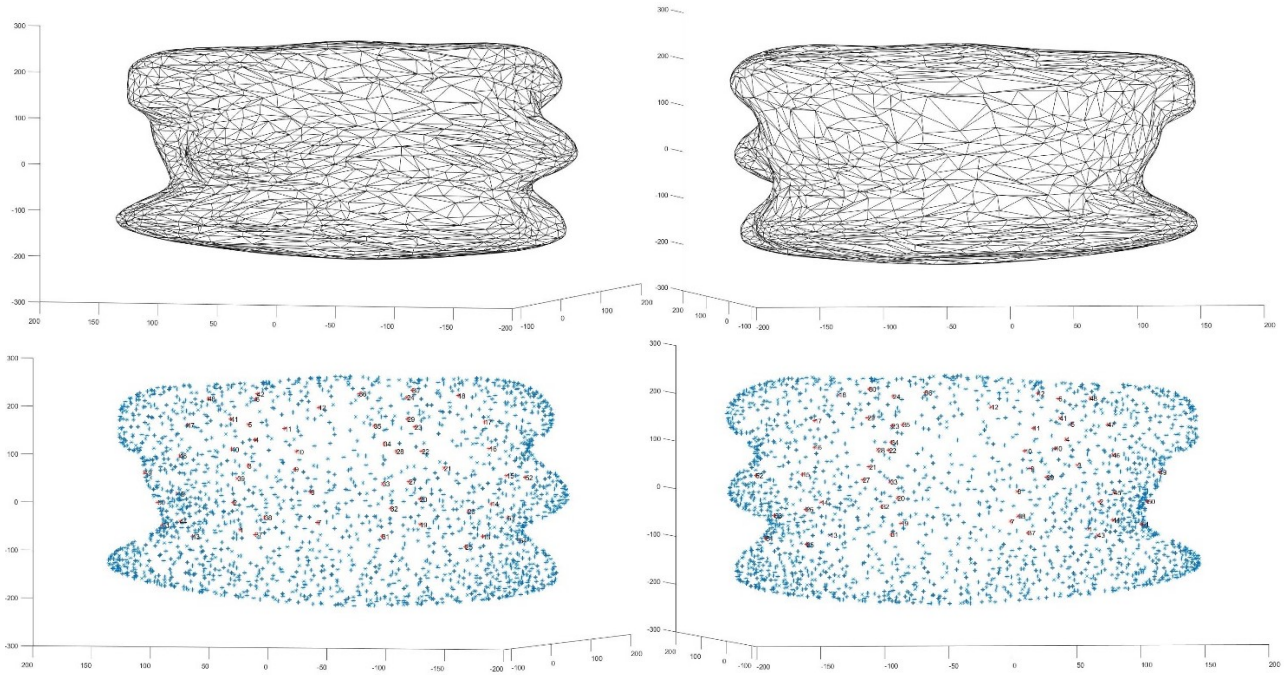

Figure 46: **Tridimensional geometries of the Torso.** Upper images represent Torso tridimensional geometry of second patient (anterior and posterior view); Lower images represent Torso tridimensional geometry of second patient (anterior and posterior view).

Table 5 shows the results of DF of SA relative to the acquisition points of the ECG recordings in the 4-10 Hz frequency band of the first patient.

ECG	**TOT**	**NEAR**	**FAR**	
	MEDIAN [25th 75th]	**MEDIAN [25th 75th]**	**MEDIAN [25th 75th]**	**P-value**
DF [Hz]	5.89 [5.72 7.52]	7.52 [7.52 7.69]	5.72 [5.48 5.89]	-
SA [%]	4239.50 [3622.80 5099.50]	4676.10 [4011.70 5378.10	4062.50 [3307.50 4746.90	0.0370

Table 5: **Results related to the ECG recordings of the first patient.** The table shows the median value **(MEDIAN)** and the **25th** and **75th** percentiles, respectively, of all the points acquired **(TOT)**, **NEAR** if the potential recorded is >7 Hz and **FAR** if <7 Hz. The values of the f waves dominant frequencies **(DF)** are expressed in Hz, instead the values of the and Spectral Area **(SA)** are expressed in %. In the last column is reported the **P-value.**

As regards the ROC analysis, a value of the *area under the curve* equal to 0.66 was obtained with an OT equal to 4246.10 V·Hz, represented in *Figure 47.*

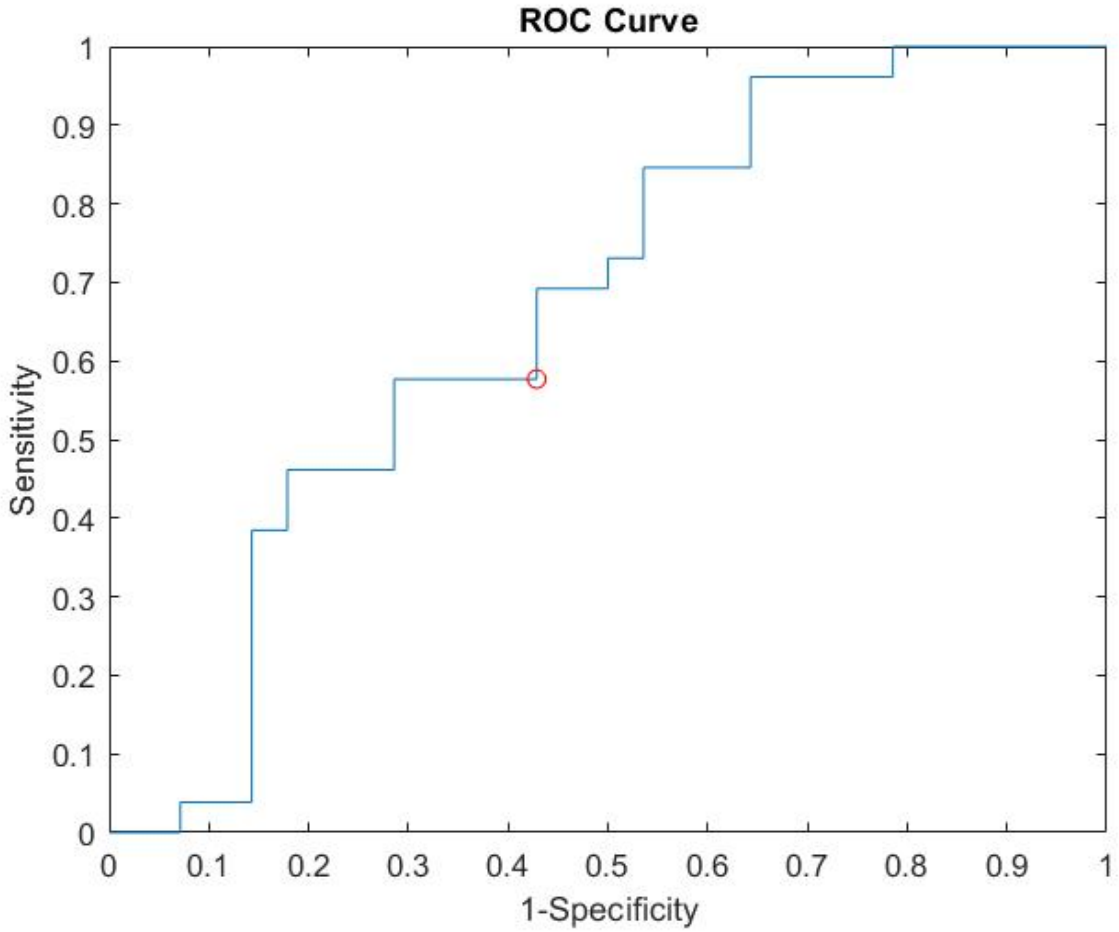

Figure 47: **ROC Curve.** The red dot indicates the optimal cut-off point relative to the f wave dominant frequency and percentage of spectrum distributions.

Figure 48 and Figure 49 show a comparison between the points on the surface of the torso, where the mapping catheter stopped during the acquisition, obtained in relation to the value of the potential recorded and the value of the and Spectral Area.

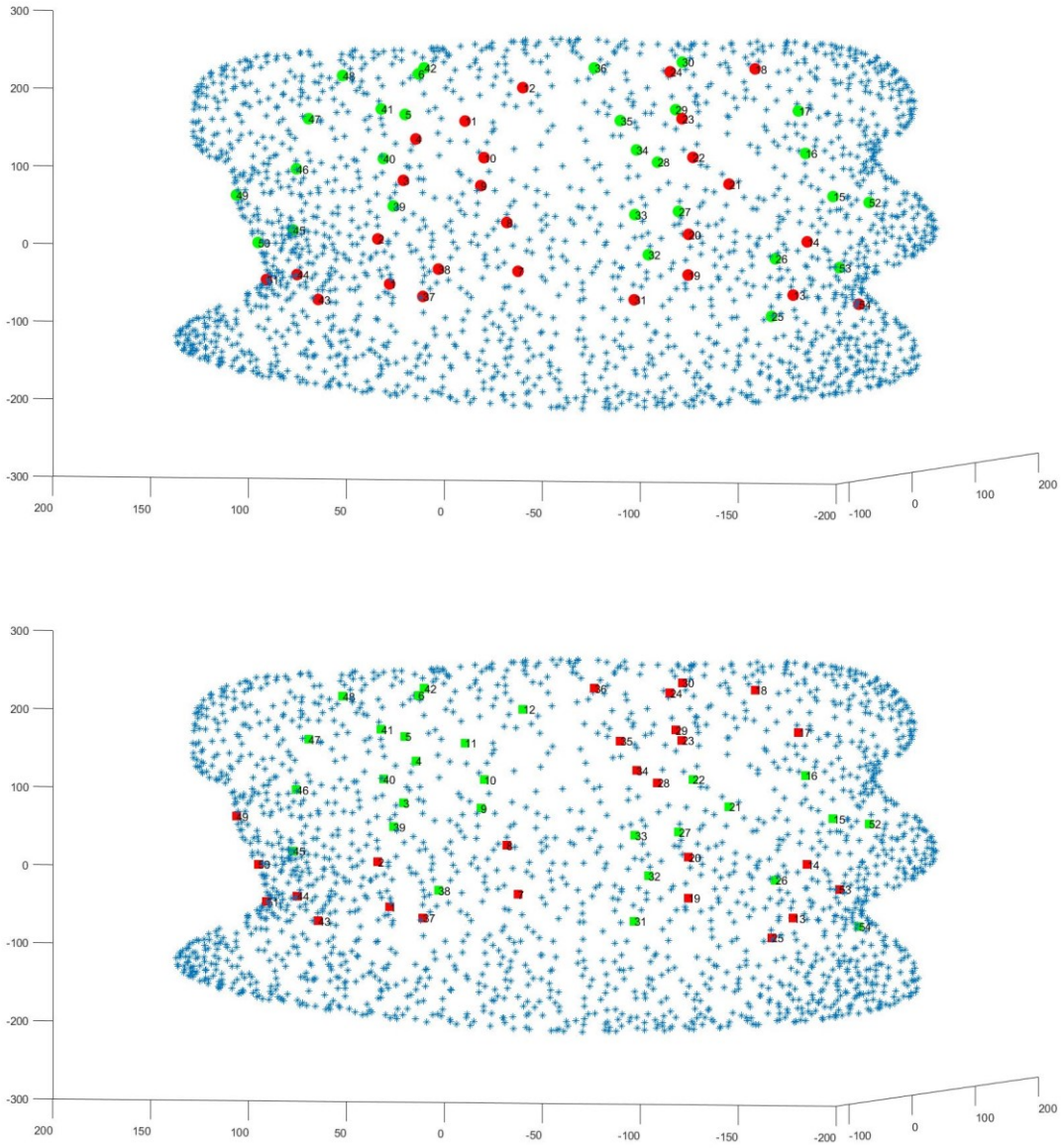

Figure 48: **Torso dominant frequency map of the second patient.** The points highlighted on the surface indicate where the mapping catheter stopped for the acquisition of information and are represented with different colors in relation to the potential value recorded: *Red* if the potential recorded is >7 Hz and *green* if <7 Hz. In the upper image there is the Torso SA map of second patient (anterior view); in the lower image there is the Torso DF map of second patient (anterior view).

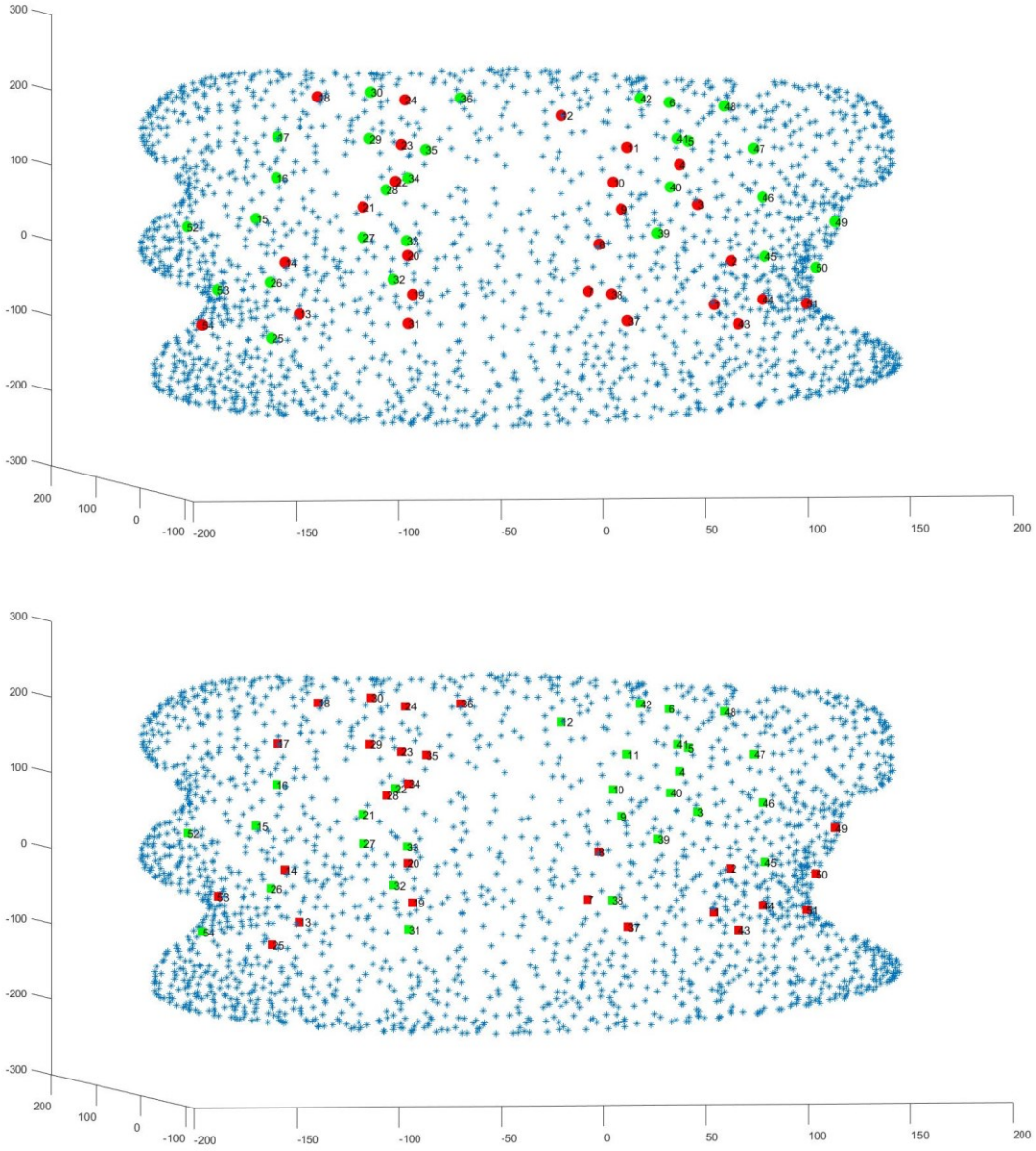

Figure 49: **Torso dominant frequency map of the second patient.** The points highlighted on the surface indicate where the mapping catheter stopped for the acquisition of information and are represented with different colors in relation to the potential value recorded: *Red* if the potential recorded is >7 Hz and *green* if <7 Hz. In the upper image there is the Torso SA map of second patient (posterior view); in the lower image there is the Torso DF map of second patient (posterior view).

5.4.3. COMPARISON BETWEEN ATRIA AND TORSO

The results of the Two One-Sided Test (TOST) applied to ECG and EGM distributions are shown in *Table 6* and *Table 7* respectively to the first and second patients.

FIRST PATIENT

	ECG			**EGM**				**TOST**
	25TH	**MEDIAN**	**75TH**	**25TH**	**MEDIAN**	**75TH**		**p-value**
DF [Hz]	6.56	6.83	6.83	6.29	6.43	7.37		6.1593e-82
SA [%]	3253.60	3828.10	4543.20	8.33	11.47	19.50		3.1902e-62

Table 6: **Statistical test result of the first patient.** The median value **(MEDIAN)** and **25th** and **75th** percentile relative to the f wave dominant frequency **(DF)** and the and Spectral Area **(SA)** respectively are shown. In the last column is present the **p-value** resulted from the test.

SECOND PATIENT

	ECG			**EGM**				**TOST**
	25TH	**MEDIAN**	**75TH**	**25TH**	**MEDIAN**	**75TH**		**p-value**
DF [Hz]	5.72	5.89	7.52	4.91	5.40	6.38		1.7580e-51
SA [%]	3622.80	4239.50	5099.50	16.95	20.07	24.28		7.4633e-73

Table 7: **Statistical test result of the second patient.** The median value **(MEDIAN)** and **25th** and **75th** percentile relative to the f wave dominant frequency **(DF)** and the and Spectral Area **(SA)** respectively are shown. In the last column is present the **p-value** resulted from the test.

5.5. DISCUSSION

In this study we tried to evaluate whether the spectral area could represent a new index, compared to the already known f wave dominant frequency, for the identification of ectopic foci during the catheter ablation procedure.

Specifically, the data set consists of the signals and geometric networks of two patients suffering from atrial fibrillation. Compared to common clinical practice, patients were given an adenosine bolus which blocks the atrioventricular node, allowing the acquisition of atrial signals without ventricular activity. This procedure was useful for the identification of f waves dominant frequency, as these waves are usually observable between QRS complexes in the frequency band between 4 and 10 Hz.

However, such a limited sample of patients represents one of the limitations of this study. Furthermore, the validity of the new index should be tested during standard clinical practices in which patients' ventricular activity is not blocked by drugs.

Specifically, the data set consists of the signals and geometric networks of two patients suffering from atrial fibrillation. Compared to common clinical practice, patients were given an adenosine bolus which blocks the atrioventricular node, allowing the acquisition of atrial signals without ventricular activity. This procedure was useful for the identification of f waves dominant frequency, as these waves are usually observable between QRS complexes in the frequency band between 4 and 10 Hz.

Regarding the atria, good results have been obtained. For each recording acquired, the dominant frequency was obtained by calculating the maximum frequency in the band between 4-10 Hz. Although it may vary from person to person, the subject's dominant frequency potential recorded was 7 Hz. In relation to this value, the acquisition points of the mapping catheter highlighted on the meshes of the atria were distinguished into near and far from potential ectopic sites. According to the literature, the results show that the dominant frequency values are greater in the regions of the right atrium, with progressively decreasing activation frequencies towards the pulmonary veins. This confirms how the f waves dominant frequency represent an index of identification of ectopic focuses.

The spectral area, on the other hand, was obtained by calculating the area of the spectrum in the frequency band between 4-10 Hz for each recording acquired. Having assumed the dominant frequencies as the gold standard and divided the points according to the recorded potential, we reconstructed the activation maps using the respective values of the spectral areas, estimating for both patients the threshold value for the distinction between far and near the potential ectopic sites. The results obtained, appear to be consistent with the activation maps of the dominant frequencies, showing values of the highest spectral areas near the right atrium, with progressively decreasing activation frequencies towards the pulmonary veins.

Regarding the reconstruction of the mapping of the body surface potential little results have been obtained. In fact, the potential maps and the maps obtained through the spectral areas are discordant. However, for clinical purposes these results are not very relevant as the classical methods of recording the surface potentials are sufficient and accurate. Instead, a good correlation

between the superficial and intracardiac potentials was obtained, which means that more studies on the inverse and direct problem of electrophysiology could lead to new and better results.

In conclusion, our study has led to good results highlighting how the spectral area of intracardiac signals can be a valid index for the identification of ectopic focuses in the presence of atrial fibrillation, less prone to disturbances and easy to calculate. Further studies and more advanced signal processing techniques could help to improve its accuracy or to discover more complex indices that perform better.

CONCLUSION AND DISCUSSION

Atrial fibrillation is one of the most common arrhythmias in the world characterized by a rapid and irregular heart rhythm, caused by the presence of multiple waves resulting from small chaotic re-entries, called ectopic foci, that occur within the atria.

Although originally applied only to relatively simple arrhythmias with a single target site, such as atrioventricular (AV) nodal reentry or tachycardias associated with Wolff-Parkinson-White syndrome, in recent years catheter ablation has been increasingly used to treat more complex arrhythmias, including atrial fibrillation.

Thanks to three-dimensional electroanatomical mapping systems, which allows to recreate the geometry of the heart chamber of interest, through an ablating catheter the surgeon is able to destroy and isolate small areas of the tissue from which the arrhythmia is triggered, in order to prevent abnormal electrical signals from spreading into the heart. It is therefore important to identify such ectopic foci to guide the ablation procedure.

One of the main indices for the identification of ectopic sites is the f wave dominant frequency, a characteristic wave of atrial fibrillation recordings presents between the QRS complexes and usually observable in the frequency band between 4-10 Hz. The f wave potential may vary from person to person. In the present study we have tried to find an alternative indicator with respect to frequencies, the area of the spectrum, that is precise and less prone to disturbances.

However, there are some limitations in this study. First of all, the evaluation of the validity of this new index was carried out with a limited sample of patients. The study should be extended to a larger population in which the threshold value of the dominant frequencies is different among the various subjects. In addition, in the present study, the two subjects were given an adenosine bolus which blocks the atrioventricular node. For this reason, the identification method should also be tested in the presence of ventricular activity, as occurs in standard ablation procedures.

In conclusion, the present study has led to good results showing how the spectral area of intracardiac signals can represent a valid index for the identification of ectopic focuses in the presence of atrial fibrillation. Specifically, it turns out to be an easy index to calculate, less prone to disturbances and much more sensitive than the dominant frequencies, as it allows to cover a wider frequency spectrum. In the present study, the frequency analysis was conducted starting from the Fast Fourier Transform, but in the future with the help of more advanced spectral analysis methods, such as self-aggressive or wavelet models, could help to improve its accuracy and achieve better performance.

BIBLIOGRAPHY

[1] B.M. Koeppen, B.A. Stanton. Berne & Levy. Physiology. 2018 Elsevier, Inc. Seventh Edition.

[2] C.L. Stanfield. Principles of Human Physiology. 2013 Pearson Education, Inc. Fifth Edition.

[3] E.P. Widmaier, H. Raff, K.T. Strang. Vander's Human Physiology: The Mechanisms of Body Function. 2016 McGraw-Hill Education. Fourteenth Edition.

[4] R.E. Klabunde. Cardiovascular Physiology Concepts. 2011 Lippincott Williams & Wilkins. Second Edition.

[5] J.J. Goldberg. Practical Signal and Image Processing in Clinical Cardiology. J.J. Goldberg, J. Ng. 2010 Springer Nature. First Edition.

[6] Manuali MSD Edizione Professionisti (msdmanuals.com)

[7] Mayo Clinic - Mayo Clinic

[8] G. Lippi, F. Sanchis-Gomar, G. Cervellin. Global epidemiology of atrial fibrillation: An increasing epidemic and public health challenge. 2021 International Journal of Stroke. 16(2):217-221.

[9] A. Raviele, M. Disertori, P. Alboni, E. Bertaglia, G. Botto, M. Brignole, R. Cappato, A. Capucci, M.D. Greco, R.D. Ponti, M.D. Biase, G.D. Pasquale, M. Gulizia, F. Lombardi, S. Themistoclakis, M. Tritto. Linee guida AIAC per la gestione e il trattamento della fibrillazione atriale. 2013 Giornale Italiano di Cardiologia. 14(3):215-240.

[10] M.K. Chung, M. Refaat, W.K. Shen, V. Kutyifa, Y.M. Cha, L. Di Biase, A. Baranchuk, R. Lampert, A. Natale, J. Fisher, D.R. Lakkireddy. Atrial Fibrillation: JACC Council Perspectives. 2020 Journal of the American College of Cardiology. 75(14):1689-1713.

[11] Electrophysiology Lab Suite – RADA (rada-arch.com)

[12] L. Roten, N. Derval, P. Pascale, D. Scherr, Y. Komatsu, A. Shah, K. Ramoul, A. Denis, F. Sacher, M. Hocini, M. Haïssaguerre, P. Jaïs. Current Hot Potatoes in Atrial Fibrillation Ablation. 2012 Current Cardiology Reviews. 8(4): 327–346.

[13] D.E. Haines, S. Beheiry, J.G. Akar, J.L. Baker, D. Beinborn, J.F. Beshai, N. Brysiewicz, C. Chiu-Man, K.K. Collins, M. Dare, K. Fetterly, J.D. Fisher, R. Hongo, S. Irefin, J. Lopez, J.M. Miller, J.C. Perry, D.J. Slotwiner, G.F. Tomassoni, E. Weiss. Heart Rhythm Society Expert Consensus Statement on Electrophysiology Laboratory Standards: Process, Protocols, Equipment, Personnel, and Safety. 2014 Heart Rhythm Society. 11(8):e9-51.

[14] S.K.S. Huang, J.M. Miller. Catheter ablation of cardiac arrhythmias. 2020 Elsevier. Fourth Edition.

[15] American Heart Association | To be a relentless force for a world of longer, healthier lives

[16] F. Stazi. Knots to untie: anticoagulant and antiarrhythmic therapy after ablation for atrial fibrillation. 2020 European Heart Journal Supplements. L136–L139.

[17] M. Anselmino, M. Matta, E. Toso, F. Ferraris, D. Castagno, M. Scaglione, F. Cesarani, R. Faletti, F. Gaita. Silent Cerebral Embolism during Atrial Fibrillation Ablation: Pathophysiology, Prevention and Management. 2013 Journal of Atrial Fibrillation. 6(2):796.

[18] S.C. Sporton, M.J. Earley, A.W. Nathan, R.J. Schilling. Electroanatomic Versus Fluoroscopic Mapping for Catheter Ablation Procedures: A Prospective Randomized Study. 2004 Journal of Cardiovascular Electrophysiology. 15(3):310-5.

[19] J. Wasserlauf, D.J. Pelchovitz, J. Rhyner, N. Verma, M Bohn, Z. Li, R. Arora, A.B. Chicos, J.J. Goldberger, S.S. Kim, A.C. Lin, B.P. Knight, R.S. Passman. Cryoballoon versus Radiofrequency Catheter Ablation for Paroxysmal Atrial Fibrillation. 2015 Pacing and Clinical Electrophysiology. 38(4):483-9.

[20] Ablation Products for Atrial Fibrillation - Pulmonary Vein Ablation Catheter (PVAC) GOLD | Medtronic

[21] Cardiac Ablation Products for Atrial Fibrillation - Arctic Front Advance Cryoablation Catheter | Medtronic

[22] D. Panescu, J.G. Whayne, S.D. Fleischman, M.S. Mirotznik, D.K. Swanson, J.G. Webster. Three-dimensional finite element analysis of current density and temperature distributions during radio-frequency ablation. 1995 IEEE Transactions on Biomedical Engineering. 42(9):879-90.

[23] S. Tungjitkusolmun, S.T. Staelin, D. Haemmerich, J.Z. Tsai, H. Cao, J.G. Webster, F.T. Lee, D.M. Mahvi, V.R. Vorperian. Finite element modeling of radio-frequency cardiac and hepatic ablation. 2001 IEEE Transactions on Biomedical Engineering. 49(1):3-9.

[24] D. Haemmerich. Biophysics of Radiofrequency Ablation. 2010 Critical Reviews in Biomedical Engineering. 38(1):53-63.

[25] F. Kreith. The CRC Handbook of Thermal Engineering, 2000 R.P. Chhabra. Second Edition. pp.114-215.

[26] K. Yokoyama, H. Nakagawa, F.H.M. Wittkampf, J.V. Pitha, R. Lazzara, W.M. Jackman. Comparison of Electrode Cooling Between Internal and Open Irrigation in Radiofrequency Ablation Lesion Depth and Incidence of Thrombus and Steam Pop. 2006 Circulation. 113:11–19

[27] D. Haemmerich, L. Chachati, A.S. Wright, D.M. Mahvi, F.T. Lee, J.G. Webster. Hepatic Radiofrequency Ablation with Internally Cooled Probes: Effect of Coolant Temperature on Lesion Size. 2003 IEEE Transactions on Biomedical Engineering, VOL. 50, NO. 4. 493 – 500.

[28] I. Cordero. Electrosurgical units – how they work and how to use them safely. 2015 Community Eye Health. 2015 Community Eye Health. 28(89): 15–16.

[29] Z. Issa, J. Miller. Clinical Arrhythmology and Electrophysiology: A Companion to Braunwald's Heart Disease. 2012 Elsevier Inc.

[30] R.D. Ponti. Cryothermal Energy Ablation Of Cardiac Arrhythmias 2005: State Of The Art. 2005 Indian Pacing and Electrophysiology Journal. 5(1):12-24.

[31] M.D. Olson, T. Nantsupawat, N. Sathnur, H. Roukoz. Cardiac Ablation Technologies. 2019 Elsevier Inc.

[32] S. Mahida, B. Berte, S. Yamashita, N. Derval, A. Denis, A. Shah, S. Amraoui, M. Hocini, M. Haissaguerre, P. Jais, F. Sacher. New Ablation Technologies and Techniques. 2014 Arrhythmia & Electrophysiology Review. 3(2):107-12.

[33] M.A. Crandall, E.G. Daoud, C.J. Daniels, S.J. Kalbfleisch. Percutaneous radiofrequency catheter ablation for atrial fibrillation prior to atrial septal defect closure. 2012 Journal of Cardiovascular Electrophysiology. 23(1):102-4.

[34] E. Seeram. Digital Fluoroscopy. Physical Principles and Quality Control. 2019 Springer, Singapore.

[35] R. Robledo-Nolasco, J.R. Leal-Díaz. Radiofrequency catheter ablation of cardiac arrhythmias using only threedimentional mapping systems. 2020 Cardiovascular and Metabolic Science.

[36] R. Stoute, M.C. Louwerse, V.A. Henneken, R. Dekker. Intravascular Ultrasound at the tip of a guidewire: Concept and first assembly steps. 2016 Elsevier Inc. Pages 1563-1567.

[37] D. Bhakta, J.M. Miller. Principles of Electroanatomic Mapping. 2008 Indian Pacing and Electrophysiology Journal. 8(1): 32-50.

[38] M. Borlich, P. Sommer. Cardiac Mapping Systems Rhythmia, Topera, EnSite Precision, and CARTO. 2019 Cardiac Electrophysiology Clinics. 11(3):449-458.

[39] EnSite Precision™ Cardiac Mapping System | Abbott Cardiovascular

[40] C. Eitel, G. Hindricks, N. Dagres, P. Sommer, C. Piorkowski. EnSite Velocity™ cardiac mapping system: a new platform for 3D mapping of cardiac arrhythmias. 2010 Expert Review of Medical Devices. 7:2, 185-192.

[41] P. Zając, Ł. Konarski, M. Wójcik. EnSite™ Precision-3D Cardiac Mapping System. 2016 European Journal of Medical Technologies.

[42] S. Pizzini. CARTO 3 system. 2017 Johnson & Johnson Medical NV/SA.

[43] R. Kabra, J. Singh. Recent Trends in Imaging for Atrial Fibrillation Ablation. 2010 Indian Pacing and Electrophysiology Journal. 10 (5): 215-227.

[44] M. Christoph, C. Wunderlich, S. Moebius, M. Forkmann, J. Sitzy, J. Salmas, J. Mayer, Y. Huo, C. Piorkowski, T. Gasparet. Fluoroscopy integrated 3D mapping significantly reduces radiation exposure during ablation for a wide spectrum of cardiac arrhythmias. 2015 Europace. 17(6):928-37.

[45] Cardiac Arrhythmia Mapping System – RHYTHMIA HDx - Boston Scientific

[46] M. Marchetti, C. Furno, L. Leogrande. Report di Valutazione di Dispositivi Medici: Sistema di Navigazione Non Fluoroscopica e Mappaggio Cardiaco ad Alta Intensità Rhythmia. 2016 Bollettino SIFO. 62(5):295-299

[47] J. Pedròn-Torrecilla, M. Rodrigo, A.M. Climent, A. Liberos, E. Pèrez-David, J. Bermejo, A. Arenal, J. Millet, F. Fernandez-Avilès, O. Berenfeld, F. Atienza, M. S. Guillem. Noninvasive Estimation of Epicardial Dominant High-Frequency Regions During Atrial Fibrillation. 2016 Journal of Cardiovascular Electrophysiology. 27(4):435-442.